ADDIS ABABA UNIVERSITY
ADDIS ABABA INSTITUTE OF TECHNOLOGY
SCHOOL OF ELECTRICAL AND COMPUTER ENGINEERING

GENETIC ALGORITHM-BASED JOINT CHANNEL ESTIMATION AND DATA DETECTION FOR MULTI-USER MIMO

By Asmamaw Getu

Thesis Submitted to the School of Electrical and Computer Engineering

Presented in Partial Fulfillment of the Degree of Masters of Science in Electrical and Computer Engineering (Communication Engineering)

Addis Ababa, Ethiopia

April 2014

Addis Ababa University
School of Graduate Studies

This is to certify that the thesis prepared by Asmamaw Getu, entitled: *Genetic Algorithm-based Joint Channel Estimation and Data Detection for Multi-user MIMO* and submitted in partial fulfillment of the requirements for the *Degree of Masters in Science (Communication Engineering)* complies with the regulations of the University and meets the accepted standards with respect to originality and quality.

Signed by the Examination Committee:

Advisor___Dr. Ing. Dereje Hailemariam___ Signature_____ Date_____

Examiner_____ Signature_____ Date_____

Examiner_____ Signature_____ Date_____

_____

Chair of Department of Graduate Program Coordinator

Declaration

I, the undersigned, declare that this MSc thesis is my original work, has not been presented for fulfillment of a degree in this or any other university, and all sources and materials used for the thesis have been acknowledged.

Name: Asmamaw Getu
Signature: _____
Place: Addis Ababa
Date of submission: _____

This thesis work has been submitted for examination with my approval as a university advisor.

Dr. Ing. Dereje Hailemariam _____

Advisor's Name Signature

Acknowledgment

First of all, I would to thank my advisor Dr.-Ing. Dereje Hailemariam. It is impossible to get this thesis without his great advice, cooperation, and fellowship.

Secondly, I want to thank my families my father, my mother, and all the others who give me their love and advice in one or another way. Finally, I would to thank all AAiT electrical and computer engineering school staffs for their cooperation.

Table of Contents

Abstract

To increase the number of users supported by a basestation, current technologies use space division multiple access (SDMA) as one of spectral efficient multiplexing method. Multi-user multiple-input multiple-output (MU-MIMO) is one of the special cases of SDMA which uses different channel estimation (CE) and data detection (DD) methods at the receiver.

In this thesis uplink cellular communication system with four simultaneous users, each occupied with a single transmitter antenna and two receiver antennas at the basestation is designed. Transmitted signals from different users are detected at the basestation receiver using their unique user specific spatial signature constituted by their frequency domain channel transfer functions (FD-CHTFs).

Accurate channel state information (CSI) is required at the receiver for coherent demodulation and interference cancelation. Due to large number of independent transmitter to receiver links CE is more challenging for MU-MIMO. Genetic algorithm (GA) is used as an effective solution to the MU-MIMO joint CE and DD problem in the above mentioned overloaded scenario.

GA-based channel estimator and GA-based data detector are designed independently using selection, crossover, mutation, and replacement operators. Optimum parameter values are selected using observation of change in fitness values with change in parameter values. Performance comparisons between different CE and DD methods are made by using bit error rate (BER) and mean square error (MSE) values at specific signal-to-noise ratio (SNR) points.

GA-based joint channel estimation and data detection (JCEDD) is designed by combining GA-based CE and GA-based DD and performance of the receiver is compared with other JCEDD methods. Reliability of the overloaded receiver is further increased by the use of low-density parity-check (LDPC) channel encoder.

Key words: MU-MIMO, Channel estimation, Multi-user detection, Genetic algorithm.

List of Acronyms

3G	Third Generation
4G	Fourth Generation
AI	Artificial Intelligence
AWGN	Additive White Gaussian Noise
BCE	Blind Channel Estimation
BER	Bit Error Rate
CDMA	Code Division Multiple Access
CE	Channel Estimation
CIR	Channel Impulse Response
CSI	Channel State Information
DD	Data Detection
DDCE	Decision Directed Channel Estimation
EA	Evolutionary Algorithm
EM	Expectation Maximization
FD-CHTF	Frequency Domain CHannel Transfer Function
FDMA	Frequency Division Multiple Access
GA	Genetic Algorithm
HSDPA	High Speed Downlink Packet Access
IEEE	International Electrical and Electronics association
JCEDD	Joint Channel Estimation and Data Detection
JCEMUD	Joint Channel Estimation and Multi-User Detection
LDPC	Low Density Parity Check
LS	Least Square
LTE	Long Term Evolution
MIMO	Multiple Input Multiple Output

MISO	Multiple Input Single Output
ML	Maximum Likelihood
MLD	Maximum Likelihood Detector
MMSE	Minimum Mean Square Error
MSE	Mean Square Error
MU-MIMO	Multi-User Multiple Input Multiple Output
MUD	Multi-User Detection
OFDM	Orthogonal Frequency Division Multiplexing
OFDMA	Orthogonal Frequency Division Multiple Access
OHRSA	Optimized Hierarchy Reduced Search Algorithm
OSIC	Ordered Successive Interference Cancelation
QRD-M	QR-Decomposition combined with the M-algorithm
SBCE	Semi-Blind Channel Estimation
SDMA	Space Division Multiple Access
SIC	Successive Interference Cancelation
SIMO	Single Input Multiple Output
SINR	Signal to Interference plus Noise Ratio
SISO	Single Input Single Output
SNR	Signal-to-Noise Ratio
SVD	Singular Value Decomposition
TBCE	Training Based Channel Estimation
TDMA	Time Division Multiple Access
UMTS	Universal Mobile Telecommunication System
Wi-Fi	Wireless Fidelity
WiMAX	Worldwide Interoperability for Microwave Access
WLAN	Wireless Local Area Network
ZF	Zero Forcing

List of Definitions

List of Figures

List of Tables

CHAPTER 1

INTRODUCTION

1.1 Background

In 1898 Marconi demonstrated the first radio transmission from the Isle of Wight to a tugboat 18 miles away, and radio communications was born. Radio technology advanced rapidly to enable transmissions over larger distances with better quality, less power, and smaller devices, thereby enabling public and private radio communications, television, and wireless networking [1].

The basic elements of a digital communication system are the information source, source encoder, channel encoder, and modulator at the transmitter block and demodulator, channel decoder, source decoder, and information sink at the receiver block. The transmission channel, which used to deliver the output of the transmitter to the receiver, is another main component of the system. The schematic diagram of a digital communication system is shown in Figure 1 [6].

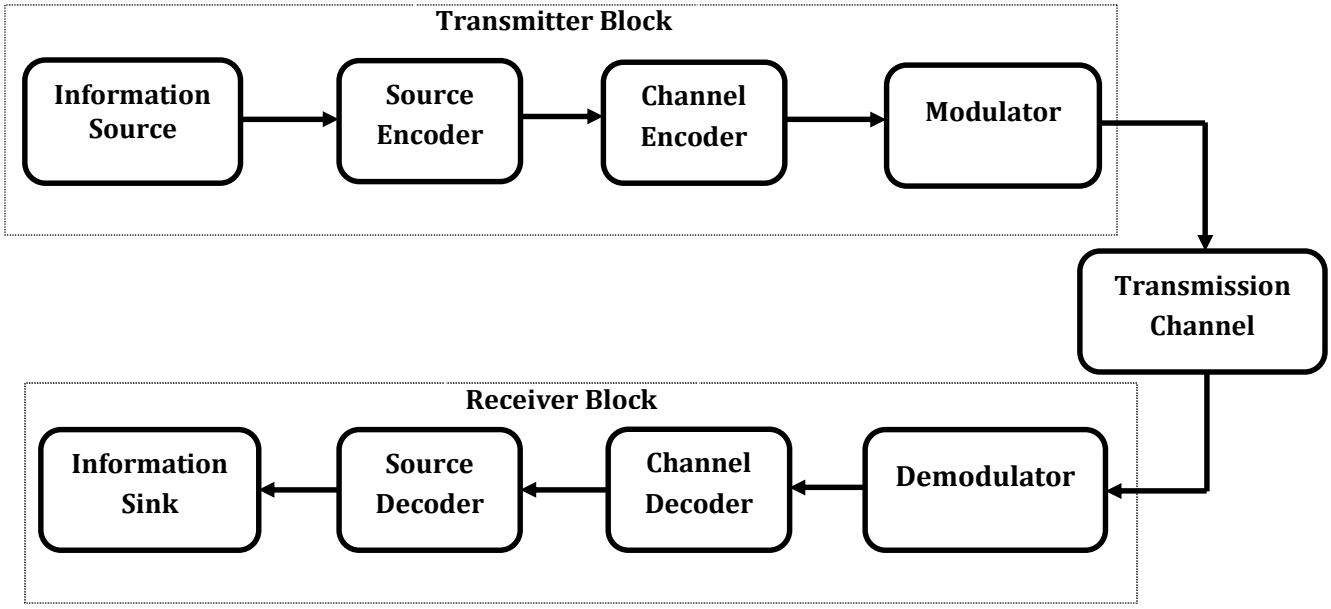

Figure 1: Block diagram of a basic digital communication system.

Of particular importance in the analysis and design of communication systems are the characteristics of the physical channels through which the information is transmitted. Design of wireless networks differs fundamentally from wired network design is due to the nature of the wireless channel. This channel is an unpredictable and the radio spectrum is a scarce resource that must be allocated to different applications and systems [6].

Multiple access schemes are used to allow many mobile users to share simultaneously a finite amount of a radio spectrum. The sharing of spectrum is required to achieve high capacity by simultaneously allocating the available bandwidth to multiple users. For high quality communications, this must be done without severe degradation in the performance of the system [3].

The use of multiple antennas at the transmitter and/or receiver ends has become one of the most important paradigms for the deployment of existing and emerging wireless communication systems. The importance of multiple input multiple output (MIMO) system is in technologies like wireless local area network (WLAN) IEEE802.11n, worldwide interoperability for microwave access (WiMAX) IEEE802.16m, and long term evolution (LTE) [7].

MIMO system is used to increase data rates through multiplexing or to improve performance through diversity. Multiplexing exploits the structure of the channel gain matrix to obtain independent signaling paths that can be used to send independent data. Spatial diversity is one of several wireless diversity schemes that use two or more antennas at the transmitter and/or receiver to improve the reliability of a wireless link. In the literature, other cases of simplified MIMO systems are also explained [14]:

- Single input multiple output (SIMO) is a simplified form of MIMO systems where the transmitter system has a single antenna.
- Multiple input single output (MISO) is a form of MIMO systems where the receiver system has a single antenna.
- When neither the transmitter nor the receiver has multiple antennas, the radio system is called single input single output (SISO) system.

Multi-user MIMO can be seen as an extended concept of space division multiple access which allows a terminal to transmit (or receive) signals to (or from) multiple users in the same frequency band simultaneously.

Consider uplink MU-MIMO system with M single antenna mobile stations (MS) and N receiver antennas at the basestation, the resulting diagram is shown on Figure 2.

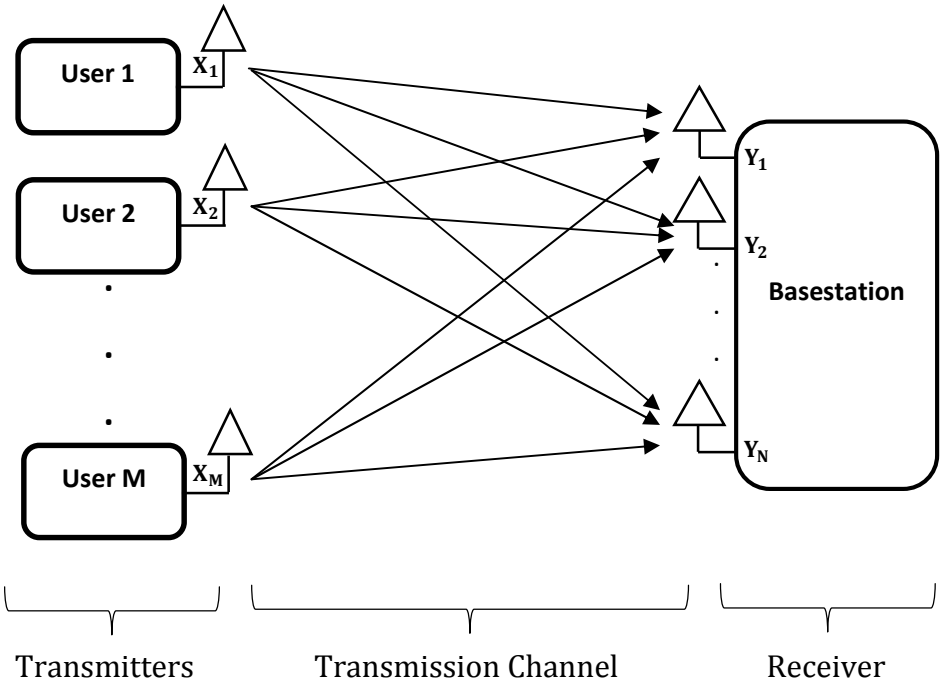

Figure 2: Uplink MU-MIMO communication system.

For uplink communication with M simultaneous mobile users, each occupied with a single transmitter antenna, and N receiver antennas at a basestation different multi-user detection (MUD) methods are employed. Transmitted signals of different users are detected using their unique user specific spatial signature constituted by their frequency domain channel transfer functions or, equivalently, channel impulse responses (CIRs).

Accurate channel state information is required at the basestation for coherent demodulation and interference cancelation. Due to large number of independent transmitter to receiver links channel estimation is more challenging for MIMO than SISO [13]. However, in the context of MU-MIMO systems, most of CE techniques found in the

literature were developed under the assumption that the number of transmitting users M is lower than or equal to the number of receiver antennas N, i.e. M≤N.

This assumption is critical for the following reasons. When M>N, which is referred to as an *overloaded scenario*, the NxM dimensional MIMO channel transfer function matrix representing the NxM number of channel links becomes *singular*, thus rendering the degree of freedom of the detector insufficient. This will catastrophically degrade the performance of multi-user detection approaches [13].

Furthermore, the associated significant degradation of the MUD's performance in this overloaded scenario will inevitably result in severe error propagation in decision directed types of basestation receivers. Genetic algorithm based joint channel estimation and data detection approach provides an effective solution to the MU-MIMO channel estimation and data detection problem mentioned in overloaded scenario.

Using GA supporting a high number of users is physically possible, because the proposed GA-based techniques dispenses with any constraints concerning the rank of the channel matrix [13].

1.2 Motivation

The main motivation of this thesis is to increase the capacity of cellular systems by using MU-MIMO concept, i.e., increase the number of simultaneous mobile stations that access the same number of basestation antennas at the same time slot and frequency band. This improvement will become possible by designing an overloaded basestation receiver using sophisticated CE and MUD methods. As a result the capacity of basestations and the overall cellular system increases remarkably.

1.2.1 Statement of the problem

To increase the capacity of cellular communication systems different multiple access methods have been used by different technologies. Some of these are frequency division multiple access (FDMA), time division multiple access (TDMA) and code division multiple access (CDMA). Current technologies use space division multiple access as one of spectral efficient multiplexing method. MU-MIMO is one of the special cases of SDMA

which uses different channel estimation and multi-user detection methods at the receiver.

There are different CE and MUD methods used at the receiver of a basestation. Least square (LS), minimum mean square error (MMSE), and decision directed based channel estimation (DDCE) methods are some of the channel estimation algorithms. Zero forcing (ZF), minimum mean square error, and maximum likelihood (ML) are the main multi-user detection methods. These CE and MUD methods are used for uplink communication where the number of transmitting users are less than or equal to the number of receiving antennas on the basestation [13].

As the number of mobile users (M) is larger than the number of receiver antennas (N) it is difficult to get the required reliability using the normal channel estimation and data detection algorithms. So it is necessary to drive new algorithm that is robust for overloaded uplink scenario. Genetic algorithm based joint channel estimation and data detection is a new candidate to overcome the problem.

The main objective of this thesis is to drive an algorithm for overloaded basestation receiver to support the required level of multiplexing gain. Genetic algorithms are the good choice for joint channel estimation and data detection of MU-MIMO uplink communication.

1.2.2 Contribution of thesis

The main contribution of this thesis is to propose GA-JCEDD that is used for overloaded receiver with smaller complexity and better performance. This will increase the capacity of the basestation by increasing the number of users that access small number of receiver antennas at the same time slot and at the same frequency band. The main works done in this thesis are:

- Design GA-JCEDD for overloaded basestation receiver.
- Compare performance and complexity of different MUD methods with GA-MUD.
- Compare performance and complexity of different CE methods with GA-CE.

1.3 Objectives of Thesis

1.3.1 Main objective

The main objective of this thesis is to increase the capacity of a cellular system by increasing the number of simultaneous users that access a basestation at the same frequency band. This is achieved by designing and simulating an overloaded MU-MIMO receiver system using sophisticated CE and MUD algorithms. One of the methods used to achieve the goal is GA. The receiver is designed using GA-JCEDD, the result is compared with other CE and MUD methods, and the performance improvement is evaluated.

1.3.2 Specific objectives

Specific objectives are:

- Design GA based MUD with full CSI and compares it with other MUD methods.
- Design GA based CE with ML MUD and compares it with other CE methods.
- Select optimum GA parameter values that decrease complexity of the receiver.
- Improve the performance of the overloaded receiver using GA-JCEDD algorithm.
- Decrease the complexity of the overloaded receiver with acceptable quality.
- Improve the reliability of the uplink communication system using channel coding.

1.4 Literature Review

As a key building block of next-generation wireless communication systems, MIMOs are capable of supporting significantly higher data rates than the universal mobile telecommunications system (UMTS) and the high-speed downlink packet access (HSDPA) based third generation (3G) networks which didn't use MIMO techniques either for diversity or for multiplexing and multiple accesses [22].

The concepts of MIMOs have been under development for many years. The earliest ideas in this field go back to work by A. R. Kaye and D. A. George (1970), Branderburg and Wyner (1974), and W. Van Etten (1975, 1976) [44]. One of the earliest MIMO applications for wireless communications dates back to 1984, when Winters published a breakthrough contribution, where he introduced a technique of optimum combining for

Rayleigh fading cellular mobile radio system [23]. Since then, Winters and others [24–30] have made further significant advances in the field of MIMOs. In 1996, Raleigh and Foschini [31] proposed new approaches for improving the efficiency of MIMO systems, which inspired numerous further contributions [32, 33].

Arogyaswami Paulraj and Thomas Kailath proposed the concept of spatial multiplexing (SM) using MIMO in 1993. Their US patent (No. 5,345,599 issued in 1994) emphasized “wireless broadcast communication applications” and “splitting a high-rate signal into several low-rate signals” [42]. The MU-MIMO concept of SDMA was proposed by Richard Roy and Bjorn Ottersten, researchers as ArrayComm, in 1991. Their US patent (No. 5515378 issued in 1996) emphasizes "an array of receiving antennas at the basestation" and "plurality of remote users" [43].

In the commercial area, Iospan Wireless Inc. developed the first commercial system in 2001 that used MIMO with orthogonal frequency-division multiple access (OFDMA) technology (MIMO-OFDMA). Iospan technology supported both diversity coding and spatial multiplexing. In 2005, Airgo Networks had developed an IEEE 802.11n precursor implementation based on their patents on MIMO. Following that in 2006, several companies (including Broadcom, Intel, and Marvell) fielded a MIMO-OFDM solution based on a pre-standard for 802.11n wireless fidelity (Wi-Fi) standard. Also in 2006, several companies (Beceem Communications, Samsung, Runcom Technologies, etc.) had developed MIMO-OFDMA based solutions for IEEE 802.16e WiMAX broadband mobile standard [46].

In the literature, a number of blind channel estimation techniques have been proposed for MIMO OFDM systems [34, 35, and 36]. However, most of these approaches suffer from either slow convergence rate or performance degradation due to the inherent limitations of blind search mechanisms. By contrast, the techniques benefiting from explicit training with the aid of known pilot signals are typically capable of achieving a better performance at the cost of a reduced effective system throughput. For example, Li et al. proposed an approach exploiting channel estimation, transmitter diversity, and the delay profile characteristics of typical mobile channels [37, 41].

Other CE schemes employed minimum mean square error [50], iterative least-squares [38], second-order statistics (SOS) based subspace estimation algorithms [48], QR-decomposition combined with the M-algorithm (QRD-M) [40], and techniques based on time of arrival (TOA) [47]. Some researchers focused their attention on designing optimum training patterns or structures [39].

The MUD methods used in most of the literatures are the linear LS and MMSE techniques, as well as nonlinear techniques, such as ML, successive interference cancelation (SIC), genetic algorithm-aided MMSE (GA-MMSE), and the novel optimized hierarchy reduced search algorithm (OHRSA) [12].

In the literature, only a few CE and MUD schemes have been proposed based on GAs. A batch blind equalization scheme is developed in 1998 based on ML joint channel and data estimation. In this scheme, the joint ML optimization is decomposed into a two level optimization loop. A micro GA is employed to identify the unknown channel model, and the Viterbi algorithm is used to provide the ML sequence estimation of the transmitted data sequence [53]. In 2001 Kai Yen and Lajos Hanzo [54] proposed a GA-aided multi-user synchronous CDMA single-antenna receiver, which jointly estimates the transmitted symbols and fading channel coefficients of all the users. The same persons Kai Yen and Lajos Hanzo did GA assisted MUD for asynchronous CDMA communications in 2004 [55].

In 2006 F. Ciriaco, T. Abraoa, and E. Jeszensky did a heuristic algorithm based on the GA based evolution theory applied to multipath multiuser channel estimation in direct sequence code division multiple access scenario [56]. At the same year M. Jiang, J. Akhtman, F. Guo, and L. Hanzo did genetic algorithm assisted iterative joint channel estimator and symbol detector for MU-MIMO OFDM system where the number of transmitter antenna is larger than the number of receiver antenna [57]. The work of M. Jiang, J. Akhtman, and L. Hanzo was published in 2007 with some modification [59].

One year later, in 2007 Hassan Ali and Dino Isa Amshah introduce a new genetic algorithm, which allows to refine the estimates of information source symbols and

channel estimates obtained by any identification algorithm [60]. Instead of searching the entire space, the proposed algorithm searches for the refined estimates in the subspaces near the initial estimate [58]. Similar works have been done by J. B. Yamindi and Prof. Wu Mu-qing in 2009 and J. Zhang, S. Chen, Xiaomin Mu, and L. Hanzo in 2011 [61].

1.5 Methodology

The methods employed to achieve the objectives of the research are:

a. Literature review:

   Include reading books, journals, articles, simulation tools, and other resources related to channel estimation, multi-user detection, and genetic algorithm.

b. System modeling:

   Involves modeling of the overall uplink system including the information source, channel encoder, and modulator at the transmitter; MU-MIMO transmission channel with AWGN at the transmission channel; and CE, MUD, and channel decoder at the receiver.

c. Simulation:

   Simulating the modeled communication system using MATLAB, and then incorporating implementations of different CE and MUD methods in to the simulated system.

d. Performance comparison:

   Include comparing the BER-SNR and MSE-SNR performance and complexity of GA and other CE and MUD methods. The composite CE-MUD methods will also be evaluated under different scenarios to see the performance complexity improvements.

e. Analysis and interpretation of the results:

   The performance improvements attained by GA based CE and MUD will be analyzed and compared with other CE and MUD methods.

1.6 Thesis Organization

The thesis is composed of six main chapters. Chapter two is about channel estimation methods and it contains MU-MIMO channel modeling, training symbol based CE, semi-blind CE, and blind CE methods. In Chapter three linear and non-linear data detection methods are discussed including ZF, MMSE, ML, and SIC based MUD methods.

Genetic algorithm will be the main topic on the fourth chapter including optimization, evolutionary computation, GA terminologies, and GA operators. The main system design with GA-CE, GA-MUD, joint GA-CEMUD, and simulation results is presented in Chapter five. The last chapter contains conclusions and recommendations for future works. At the end references are included.

CHAPTER 2

CHANNEL ESTIMATION

2.1 Introduction

In most digital communication systems the source data is encoded and modulated before transmission. The transmitted signal is always distorted by the wireless transmission channel. In order to recover the transmitted bits, the channel effect must be estimated and compensated at the receiver.

In spite of immense interest from both the academic and industrial communities, a practical MIMO transceiver architecture, capable of approaching channel capacity boundaries in realistic channel conditions, remains largely an open problem. In particular, robust and accurate channel estimation in MIMO systems constitutes a major issue, preventing technologies from achieving the high capacities predicted by the relevant theoretical analysis.

2.1.1 Definition

Inorder to attain the advantages of MIMO systems, it is necessary that the receiver and/or transmitter have access channel state information. Hence, effective channel estimation algorithms are needed to guarantee the performance of communication.

Definition 1: Channel state information

Channel state information refers to known channel properties of a communication link. This information describes how a signal propagates from the transmitter to the receiver and represents the combined effect of refflection, diffraction, scattering, fading, and power decay with distance.

Inorder to choose the channel estimation technique for the MU-MIMO communication system under consideration, different aspects of implementations including the required performance, computational complexity, and time-variation of the channel must be taken into account.

2.1.2 Types of channel estimators

Many channel estimation algorithms have been developed in recent years. In the literature [34-41], three classes of methods to estimate the channel response are presented. They include training-based channel estimation (TBCE) schemes relying on training sequences that are known to the receiver, blind channel estimation (BCE) methods identifying channel only from the received sequences, and semi-blind channel estimation (SBCE) approaches as a combination of the two aforementioned procedures.

For pure TBCE schemes, a long training is necessary in order to obtain a reliable MIMO channel estimate, which reduces the system bandwidth efficiency considerably. Blind methods, that do not require any training symbols, achieve high system throughput with high computational complexity.

Semi-blind schemes require less computational complexity than blind methods and fewer training symbols than training-based methods, making them attractive for practical implementation. TBCE algorithms use only the training sequences to perform channel estimation, whereas a SBCE algorithm takes the data symbols also into account.

2.2 Channel Modeling

From a technical point of view, the greatest distinction between wireless communications and wireline communications lies in the physical properties of wireless channels. These physical properties can be described in terms of several distinct phenomena, including ambient noise, propagation losses, multipath, interference, and properties arising from the use of multiple antennas [2].

2.2.1 Wireless channel

The mechanisms behind electromagnetic wave propagation are diverse, but can generally be attributed to reflection, diffraction, and scattering. Most cellular radio systems operate in urban areas where there is no direct line of sight path between the transmitter and the receiver, and where the presence of high rice buildings causes severe diffraction loss. Due to multiple reflections from various objects, the electromagnetic waves travel along different paths of varying lengths. The interaction

between these waves causes *multipath fading* at a specific location, and the strengths of the waves decrease as the distance between the transmitter and the receiver increases [3].

Propagation models have traditionally focused on predicting the average received signal strength at a given distance from the transmitter, as well as the variability of the signal strength in cloth spatial proximity to a particular location. Propagation models that predict the mean signal strength for an arbitrary transmitter-receiver separation distance are useful in estimating the radio coverage area of a transmitter and are called *large scale propagation models*. On the other hand, propagation models that characterize the rapid fluctuations of the received signal strength over very short travel distance or short time durations are called *small scale or fading models* [3].

The transmission channel in this thesis is assumed to be *flat and slowly fading*. If the mobile radio channel has a constant gain and linear phase response over a bandwidth greater than the bandwidth of the transmitted signal, then the received signal will undergo flat fading. This type of fading is the most common type of fading described in the technical literatures [3].

In a slow fading channel, the channel impulse response changes at a rate much slower than the transmitted baseband signal. In this case, the channel may be assumed to be static over one or several bit intervals. In frequency domain, this implies that the Doppler spread of the channel is much less than the bandwidth of the baseband signals [3].

In mobile radio channels, the Rayleigh distribution is commonly used to describe the statistical time varying nature of the received envelope of flat fading signal, or the envelope of an individual multipath component. It is well known that the envelope of the sum of two Quadrature Gaussian noise signals obeys a Rayleigh distribution. The Rayleigh distribution has a probability density function (pdf) given by Equation (2.1).

$$P(r) = \begin{cases} \frac{r}{\sigma^2} \exp\left[\frac{-r^2}{2\sigma^2}\right], & 0 \le r \le \infty \\ 0, & r < 0 \end{cases} \tag{2.1}$$

Where σ is the rms value of the received voltage signal before envelope detection, and σ^2 is the time average power of the received signal before envelope detection [3].

2.2.2 MU-MIMO channel model

Based on the components they consist of there are four types of channel models in the literatures [6]. These are binary symmetric channel, discrete memoryless channel, discrete input continuous output channel, and waveform channel. In waveform channel the modulator and the demodulator are separated from the physical channel and the inputs and the outputs of the channel are waveforms.

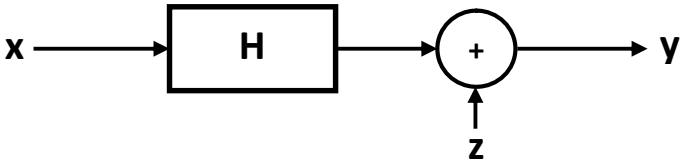

Figure 3: Waveform channel model.

Consider a MU-MIMO system equipped with M users with single transmitter antenna at the mobile station and N receiver antennas at the basestation as shown in Figure 2. Let **H** denote FD-CTF matrix with (i, j)th entry h_{ij} for the channel gain between the jth transmitter antenna and the ith receiver antenna, j=1, 2 … M and i=1, 2 ... N.

$$\mathbf{H} = \begin{bmatrix} h_{11} & h_{12} & \cdots & h_{1M} \\ h_{21} & h_{22} & \cdots & h_{2M} \\ \vdots & \vdots & \ddots & \vdots \\ h_{N1} & h_{N2} & \cdots & h_{NM} \end{bmatrix} \tag{2.2}$$

The multi-user transmitted signals and the corresponding received signals are represented by Equation (2.3) and Equation (2.4) respectively.

$$\mathbf{x} = [x_1, x_2 \ldots x_M]^T \tag{2.3}$$

$$\mathbf{y} = [y_1, y_2 \ldots y_N]^T \tag{2.4}$$

$$\mathbf{z} = [z_1, z_2 \ldots z_N]^T \tag{2.5}$$

Where x_j and y_i denote the transmit signal from the jth transmitter antenna and the received signal at the ith receiver antenna, respectively. Let z_i on Equation (2.5) denotes the white Gaussian noise with a variance of σ_z^2 at the ith receiver antenna, and $\mathbf{h_j}$ denote the jth column vector of the channel matrix. Now, the MxN MU-MIMO system is represented on Figure 4.

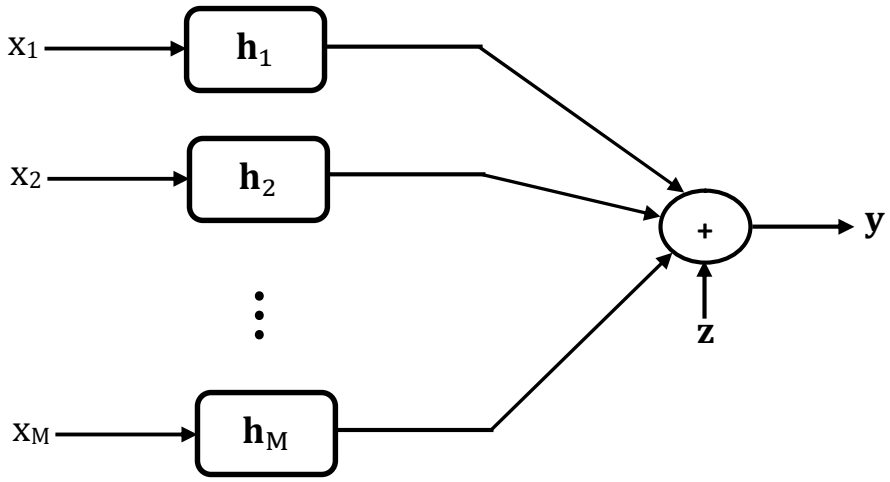

Figure 4: Channel model for MU-MIMO system.

Equation (2.6) is used to represent mathematical model of MU-MIMO system given on Figure 4. Where $\mathbf{h}_j = [h_{1j}, h_{2j} \dots h_{Nj}]^T$ and it represents the channels from transmitter antenna j to all receiver antennas for j=1, 2 … M.

$$\mathbf{y} = \mathbf{Hx} + \mathbf{z} = \mathbf{h}_1 x_1 + \mathbf{h}_2 x_2 + \dots + \mathbf{h}_M x_M + \mathbf{z} \tag{2.6}$$

Equation (2.6) can be represented in matrix form on Equation (2.7).

$$\begin{bmatrix} y_1 \\ y_2 \\ \vdots \\ y_N \end{bmatrix} = \begin{bmatrix} h_{11} & h_{12} & \cdots & h_{1M} \\ h_{21} & h_{22} & \cdots & h_{2M} \\ \vdots & \vdots & \ddots & \vdots \\ h_{N1} & h_{N2} & \cdots & h_{NM} \end{bmatrix} * \begin{bmatrix} x_1 \\ x_2 \\ \vdots \\ x_M \end{bmatrix} + \begin{bmatrix} z_1 \\ z_2 \\ \vdots \\ z_N \end{bmatrix} \tag{2.7}$$

2.3 Training Symbol-based CE

One of the most usual approaches to identify MIMO CSI is TBCE method. In this scheme, the channel is estimated based on the received pilot signals ($\mathbf{Y}_p$) and the knowledge of training symbols ($\mathbf{X}p$) during training symbol transmission period. Using Equation (2.6) the relation between $\mathbf{X_p}$ and $\mathbf{Y_p}$ is given in Equation (2.8).

$$\mathbf{Y_p} = \mathbf{HX_p} + \mathbf{Z} \tag{2.8}$$

TBCE schemes can be optimal at high signal-to-noise ratios (SNRs), but they are suboptimal at low SNRs. The optimal choice of training signals is usually investigated by minimizing mean square error (MSE) of the linear MU-MIMO channel estimator. It is

perceived that optimal design of training sequences for MIMO channel estimation is connected with the channel statistical characteristics, such as the fading model and the channel noise model [51].

Training symbols can be used for channel estimation, usually providing a good performance. However, their transmission efficiencies are reduced due to the required overhead of training symbols such as preamble or pilot tones that are transmitted in addition to data symbols. The least square and minimum mean square error techniques are widely used for channel estimation when training symbols are available [12].

2.3.1 LS CE method

LS channel estimation method finds the channel estimate $\widehat{\mathbf{H}}$ in such a way that the cost function in Equation (2.9) is minimized [12]:

$$J(\widehat{\mathbf{H}})=|\mathbf{Y} - \widehat{\mathbf{H}}\mathbf{X}|^2 = (\mathbf{Y} - \widehat{\mathbf{H}}\mathbf{X})^H(\mathbf{Y} - \widehat{\mathbf{H}}\mathbf{X}) = \mathbf{Y}^H\mathbf{Y} - \mathbf{Y}^H\widehat{\mathbf{H}}\mathbf{X} - \mathbf{X}^H\widehat{\mathbf{H}}^H\mathbf{Y} + \mathbf{X}^H\widehat{\mathbf{H}}^H\widehat{\mathbf{H}}\mathbf{X} \quad (2.9)$$

Where:

- $\mathbf{X} = [\mathbf{x}_{p1}, \mathbf{x}_{p2} \dots \mathbf{x}_{pT}]$ and $\mathbf{x}_{pt}$ is transmitted pilot signal vector for t=1, 2 … T
- $\mathbf{Y} = [\mathbf{y}_{p1}, \mathbf{y}_{p2} \dots \mathbf{y}_{pT}]$ and $\mathbf{y}_{pt}$ is received pilot signal vector for $\mathbf{y}_{pt} = \mathbf{H}\mathbf{x}_{pt} + \mathbf{z}$
- T is total number of training symbols per transmitter in one block of data
- $\mathbf{X}^H$ describes Hermitian transpose of matrix $\mathbf{X}$

For NxM transmission channel $\mathbf{H}$ and T training symbols per transmission antenna, the transmitted training signal $\mathbf{X}$ is MxT matrix and the resulting received signal will be (NxM)(MxT) = NxT matrix. By setting derivative of the cost function, J, equals to zero Equation (2.9) can be represented to Equation (2.10).

$$\frac{\partial J(\widehat{H})}{\partial \widehat{H}} = -2(\mathbf{X}^H\mathbf{Y})^* + 2(\mathbf{X}^H\widehat{\mathbf{H}}\mathbf{X})^* = 0 \text{ at } \widehat{\mathbf{H}}=\widehat{\mathbf{H}}_{LS} \quad (2.10)$$

We have $\mathbf{X}^H\widehat{\mathbf{H}}_{LS}\mathbf{X} = \mathbf{X}^H\mathbf{Y}$, which gives the solution to the LS channel estimation as given in Equation (2.11) below.

$$\widehat{\mathbf{H}}_{LS} = (\mathbf{X}^H)^{-1}\mathbf{X}^H\mathbf{Y}\mathbf{X}^{-1} = \mathbf{Y}\mathbf{X}^{-1} \quad (2.11)$$

The MSE representation of LS channel estimation method is given as MSE = $E\{|e|^2\}$ which described in Equation (2.12).

$$MSE = E\{(\mathbf{H} - \widehat{\mathbf{H}}_{LS})^H(\mathbf{H} - \widehat{\mathbf{H}}_{LS})\} \quad (2.12)$$

Substituting Equation (2.11) in to Equation (2.12) gives:

MSE = $E\{(\mathbf{H} - \mathbf{YX}^{-1})^H(\mathbf{H} - \mathbf{YX}^{-1})\}$, but $\mathbf{H} - \mathbf{YX}^{-1} = -\mathbf{ZX}^{-1}$

$= E\{(\mathbf{X}^{-1})^H(\mathbf{Z}^H\mathbf{Z})\mathbf{X}^{-1}\}$, variance of matrix $\mathbf{Z}$ is $\sigma_{\mathbf{Z}}^2 = E\{\mathbf{Z}^H\mathbf{Z}\}$

$= E\{(\mathbf{X}^H\mathbf{X})^{-1}\sigma_{\mathbf{Z}}^2\} = (E\{\mathbf{X}^H\mathbf{X}\})^{-1}\sigma_{\mathbf{Z}}^2$, variance of matrix $\mathbf{X}$ is $\sigma_{\mathbf{X}}^2 = E\{\mathbf{X}^H\mathbf{X}\}$

$= \sigma_{\mathbf{Z}}^2/\sigma_{\mathbf{X}}^2$

$$MSE = \frac{\sigma_{\mathbf{Z}}^2}{\sigma_{\mathbf{X}}^2} \quad (2.13)$$

Note that the MSE in Equation (2.13) is inversely proportional to the SNR $=\sigma_{\mathbf{X}}^2/\sigma_{\mathbf{Z}}^2$, which implies that it may be subject to noise enhancement, especially when the channel is in a deep null. For T=M, where $\mathbf{X}$ is square matrix, it is easy to determine the inverse of $\mathbf{X}$ without distortion and the LS method gives the best result. Due to its simplicity, the LS method has been widely used for channel estimation.

2.3.2 MMSE CE method

Consider the LS solution in Equation (2.11), $\widehat{\mathbf{H}}_{LS} = \mathbf{YX}^{-1} = \widetilde{\mathbf{H}}$. Using the weight matrix $\mathbf{W}$, define $\widehat{\mathbf{H}}_{MMSE} \equiv \mathbf{W}\widetilde{\mathbf{H}}$, which corresponds to the MMSE channel estimate. Referring to Figure 5, MSE of the MMSE channel estimate is given in Equation (2.14) which used as a cost function [12].

$$J(\widehat{\mathbf{H}}) = E\{|\mathbf{e}|^2\} = E\{|\mathbf{H} - \widehat{\mathbf{H}}|^2\} \quad (2.14)$$

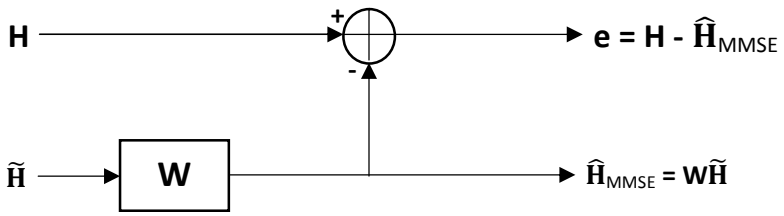

Figure 5: MMSE channel estimator.

The MMSE channel estimation method finds a linear estimate in terms of **W** in such a way that the MSE in Equation (2.14) is minimized. The orthogonality principle states that the estimation error vector $\mathbf{e} = \mathbf{H} - \widehat{\mathbf{H}}_{MMSE}$ is orthogonal to $\widetilde{\mathbf{H}}$, such that:

$$E\{\mathbf{e}\widetilde{\mathbf{H}}^H\} = E\{(\mathbf{H} - \widehat{\mathbf{H}}_{MMSE})\widetilde{\mathbf{H}}^H\} = 0$$

$$= E\{(\mathbf{H} - \mathbf{W}\widetilde{\mathbf{H}})\widetilde{\mathbf{H}}^H\}$$

$$= E\{\mathbf{H}\widetilde{\mathbf{H}}^H\} - \mathbf{W}E\{\widetilde{\mathbf{H}}\widetilde{\mathbf{H}}^H\}$$

$$= \mathbf{R}_{\mathbf{H}\widetilde{\mathbf{H}}} - \mathbf{W}\mathbf{R}_{\widetilde{\mathbf{H}}\widetilde{\mathbf{H}}}$$

$$E\{\mathbf{e}\widetilde{\mathbf{H}}^H\} = \mathbf{R}_{\mathbf{H}\widetilde{\mathbf{H}}} - \mathbf{W}\mathbf{R}_{\widetilde{\mathbf{H}}\widetilde{\mathbf{H}}} = 0 \quad (2.15)$$

Where $\mathbf{R}_{\mathbf{AB}}$ is the cross-correlation matrix of NxN matrixes **A** and **B** (i.e. $\mathbf{R}_{\mathbf{AB}}=E\{\mathbf{AB}^H\}$). From relation $\mathbf{Y} = \mathbf{HX} + \mathbf{Z}$ and Equation (2.11) LS channel estimate, $\widetilde{\mathbf{H}}$, is given in Equation (2.16).

$$\widetilde{\mathbf{H}} = \widehat{\mathbf{H}}_{LS} = \mathbf{YX}^{-1} = \mathbf{H} + \mathbf{ZX}^{-1} \quad (2.16)$$

Solving Equation (2.15) for **W** yields:

$$\mathbf{W} = \mathbf{R}_{\mathbf{H}\widetilde{\mathbf{H}}}\mathbf{R}_{\widetilde{\mathbf{H}}\widetilde{\mathbf{H}}}^{-1} \quad (2.17)$$

Where $\mathbf{R}_{\widetilde{\mathbf{H}}\widetilde{\mathbf{H}}}$ is the autocorrelation matrix of $\widetilde{\mathbf{H}}$ given as:

$$\mathbf{R}_{\widetilde{\mathbf{H}}\widetilde{\mathbf{H}}} = E\{\widetilde{\mathbf{H}}\widetilde{\mathbf{H}}^H\}$$

$$= E\{(\mathbf{YX}^{-1})(\mathbf{YX}^{-1})^H\}$$

$$= E\{(\mathbf{H} + \mathbf{ZX}^{-1})(\mathbf{H} + \mathbf{ZX}^{-1})^H\}$$

$$= E\{\mathbf{HH}^H + \mathbf{H}(\mathbf{X}^{-1})^H\mathbf{Z}^H + \mathbf{ZX}^{-1}\mathbf{H}^H + \mathbf{ZX}^{-1}(\mathbf{X}^{-1})^H\mathbf{Z}^H\}$$

$$= E\{\mathbf{HH}^H\} + E\{\mathbf{ZX}^{-1}(\mathbf{X}^{-1})^H\mathbf{Z}^H\}$$

But $E\{\mathbf{ZX}^{-1}(\mathbf{X}^{-1})^H\mathbf{Z}^H\} = E\{\mathbf{Z}(\mathbf{XX}^H)^{-1}\mathbf{Z}^H\} = \sigma_{\mathbf{Z}}^2/\sigma_{\mathbf{X}}^2$.

$$\mathbf{R}_{\widetilde{\mathbf{H}}\widetilde{\mathbf{H}}} = E\{\mathbf{HH}^H\} + \frac{\sigma_{\mathbf{Z}}^2}{\sigma_{\mathbf{X}}^2}\mathbf{I} \quad (2.18)$$

And $\mathbf{R}_{\mathbf{H}\tilde{\mathbf{H}}}$ is the cross-correlation matrix between the true CTF matrix $\mathbf{H}$ and temporary channel estimate vector in the frequency domain $\tilde{\mathbf{H}}$. Using Equation (2.17), the MMSE channel estimate is given as follows:

$$\hat{\mathbf{H}}_{\text{MMSE}} = \mathbf{W}\tilde{\mathbf{H}} = \mathbf{R}_{\mathbf{H}\tilde{\mathbf{H}}}\mathbf{R}_{\tilde{\mathbf{H}}\tilde{\mathbf{H}}}^{-1}\tilde{\mathbf{H}} \tag{2.19}$$

$\hat{\mathbf{H}}_{\text{MMSE}} = \mathbf{R}_{\mathbf{H}\tilde{\mathbf{H}}}(\mathbf{R}_{\mathbf{HH}} + \frac{\sigma_Z^2}{\sigma_X^2}\mathbf{I})^{-1}\tilde{\mathbf{H}}$, assume E[$\mathbf{H}$] = 0 and the noise is additive white gaussian noise (AWGN).

$$\hat{\mathbf{H}}_{\text{MMSE}} = (\sigma_z^2\mathbf{R}_{\text{HH}}^{-1} + \mathbf{X}^{\text{H}}\mathbf{X})^{-1}\mathbf{X}^{\text{H}}\mathbf{Y} \tag{2.20}$$

2.4 Other CE Methods

2.4.1 Decision-directed CE

Once initial channel estimation is made with the training signals, the coefficients of channel can be updated with decision-directed channel estimation, which does not use the training signals. The decision-directed technique uses the detected signal feedback to track the possibly time-varying channel while subsequently using the channel estimate to detect the signal.

In decision-directed process, any error in the detected symbol is propagated to degrade its performance. Further performance degradation is expected under fast fading, which is when channel variation is faster as compared to the OFDM symbol period. In this case, the performance degradation can be mitigated to some degree by taking the weighted average of the channel estimates between adjacent subcarriers or successive OFDM symbols [12].

2.4.2 Expectation-maximization algorithm-based CE

The expectation-maximization (EM) algorithm has been widely used in a large number of areas that deal with unknown factors affecting the outcome, such as signal processing, genetics, econometric, clinical, and sociological studies. The EM-based channel estimation is an iterative technique for finding maximum likelihood estimates of

a channel. It is classified as a semi-blind method since it can be implemented when transmit symbols are not available [13].

Despite the advantages of the EM algorithm, its application to the channel estimation of MIMO systems is not straightforward, because the computational complexity of the EM algorithm increases exponentially with the number of transmitted signals or the size of the constellation. Furthermore, EM algorithm is not applicable to a time-varying channel.

There have been some attempts to reduce the computational complexity and to improve the performance of the EM algorithm. For example, a decision-directed EM (DDEM) estimation technique has been proposed by combining the EM algorithm with the decision-directed channel estimation, which presents a reduced computational complexity in slowly time varying channels [12].

2.4.3 Blind CE

In recent years, blind estimation of MIMO linear channels has become a well-known research problem in multi-channel communications and signal recovery. Satisfactory solutions of this problem can find diverse applications in areas such as multi-user detection, array signal processing, speech processing, and multichannel biomedical signal recovery [12].

The key objective of blind MIMO channel estimation is to determine the unknown matrix channel impulse response without direct training or knowledge of the channel input signals. The receiver must rely on the statistical information from the channel output signals.

When the channel is a memoryless system, the problem is often known as blind source separation (or independent component analysis) with the goal of directly extracting source signals from the instantaneous mixtures without explicitly identifying the mixing matrix.

The BCE methods can be classified into higher-order statistics (HOS)-based techniques and second order statistics (SOS)-based techniques. Blind algorithms typically require longer data records and entail higher complexity [14].

CHAPTER 3

DATA DETECTION

3.1 Introduction

MU-MIMO system transmits different users' data using each transmitter antenna arrays. One of the key challenges in designing multi-user communication systems is mitigating interference due to multi-user data streams reached at the receiver at the same time.

In SDMA the receivers for all transmitters are co-located. Hence instead of detecting the transmitted signals from a particular user in isolation, treating the other signals as background noise, the receiver can jointly detect all of the transmitted information symbols. In that case, the structure of the multiple access interference can be used to aid the detection of the desired symbols.

Definition 2: Multi-user detection

Multiuser detection refers to the scenario in which a single receiver jointly detects multiple simultaneous transmissions.

Closely related to multiuser detection is *interference suppression*. The key distinction is that a multi-user detector attempts to retrieve multiple transmitted signals, or information streams, whereas interference suppression implies that the receiver is interested in only one signal among the received superposition of transmitted signals.

In general, a receiver may wish to demodulate a subset of two or more signals from among a larger mix of signals. In that case, the receiver jointly detects the subset of desired signals while suppressing the interfering signals [15].

There are different MUD methods which used to estimate the transmitted data signals $\hat{\mathbf{x}}$ using received signals $\mathbf{y}$ and estimated CTF matrix $\widehat{\mathbf{H}}$. The block diagram that describes the CE and MUD phase of the receiver device is given on Figure 6.

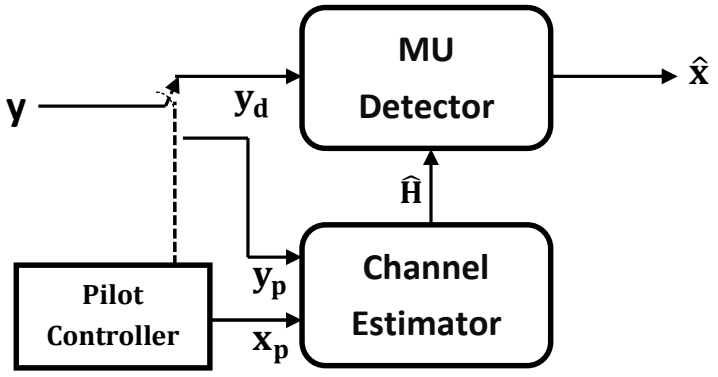

Figure 6: Structure of a receiver with CE and MUD.

3.2 Linear MUD Methods

Linear signal detection method treats all transmitted signals as interferences except for the desired stream from the target transmitter antenna. Therefore, interference signals from other transmit antennas are minimized or nullified in the course of detecting the desired signal from the target transmit antenna. To facilitate the detection of desired signals from each antenna, the effect of the channel is inverted by a weight matrix **W** such that:

$$\hat{\mathbf{x}} = \mathbf{W}\mathbf{y} \tag{3.1}$$

That is, detection of each symbol is given by a linear combination of the received signals. The standard linear detection methods include the zero-forcing (ZF) technique and the minimum mean square error (MMSE) technique [12].

3.2.1 ZF signal detection

The zero-forcing technique nullifies the interference by the weight matrix given in Equation (3.2)[1]. In other words, it inverts the effect of channel as given in Equation (3.3) [12].

$$\mathbf{W}_{ZF} = (\mathbf{H}^H\mathbf{H})^{-1}\mathbf{H}^H \tag{3.2}$$

$$\hat{\mathbf{x}}_{ZF} = \mathbf{W}_{ZF}\mathbf{y} = \mathbf{x} + (\mathbf{H}^H\mathbf{H})^{-1}\mathbf{H}^H\mathbf{z} = \mathbf{x} + \hat{\mathbf{z}}_{ZF} \tag{3.3}$$

[1] $(\mathbf{A})^H$ denotes the Hermitian transpose operation

Where $\hat{\mathbf{Z}}_{ZF} = (\mathbf{H}^H\mathbf{H})^{-1}\mathbf{H}^H\mathbf{Z}$. Note that the error performance is directly connected to the power of $\hat{\mathbf{Z}}_{ZF}$ (i.e. $|\hat{\mathbf{Z}}_{ZF}|_2^2$)[2]. Using the singular value decomposition (SVD) of $\mathbf{H}$, i.e. $\mathbf{H} = \mathbf{U\Sigma V}^H$, the post-detection noise power can be evaluated as follows.

$|\hat{\mathbf{Z}}_{ZF}|_2^2 = (\hat{\mathbf{Z}}_{ZF})^H(\hat{\mathbf{Z}}_{ZF}) = |(\mathbf{H}^H\mathbf{H})^{-1}\mathbf{H}^H\mathbf{Z}|^2$

$= |(\mathbf{V\Sigma}^H\mathbf{U}^H\mathbf{U\Sigma V}^H)^{-1}\mathbf{V\Sigma U}^H\mathbf{Z}|^2$, but $\mathbf{U}^H\mathbf{U}=\mathbf{I}$ and $\mathbf{\Sigma}^H\mathbf{\Sigma}=\mathbf{\Sigma}^2$

$= |(\mathbf{V\Sigma}^2\mathbf{V}^H)^{-1}\mathbf{V\Sigma U}^H\mathbf{Z}|^2$, $\mathbf{V}^{-1}=\mathbf{V}^H$

$= |\mathbf{V\Sigma}^{-2}\mathbf{V}^H\mathbf{V\Sigma U}^H\mathbf{Z}|^2$, $\mathbf{V}^H\mathbf{V}=\mathbf{I}$

$$|\hat{\mathbf{Z}}_{ZF}|_2^2 = |\mathbf{V\Sigma}^{-1}\mathbf{U}^H\mathbf{Z}|^2 \tag{3.4}$$

Since $|\mathbf{Qx}|^2 = (\mathbf{Qx})^H(\mathbf{Qx}) = \mathbf{x}^H\mathbf{Q}^H\mathbf{Qx} = \mathbf{x}^H\mathbf{x} = |\mathbf{x}|^2$ for a unitary matrix $\mathbf{Q}$, the expected value of the noise power is given in Equation (3.5) below.

$E\{|\hat{\mathbf{Z}}_{ZF}|_2^2\} = E\{|\mathbf{V\Sigma}^{-1}\mathbf{U}^H\mathbf{Z}|^2\}$

$= {}^3E\{tr(\mathbf{\Sigma^{-1}U^Hzz^HU(\Sigma^{-1})}^H)\}$

$= tr(\mathbf{\Sigma^{-1}U^HE\{zz^H\}U(\Sigma^{-1})}^H)$, $\sigma_z^2 = \mathbf{E\{zz^H\}}$

$= tr(\sigma_z^2\mathbf{\Sigma^{-1}U^HU(\Sigma^{-1})}^H)$, $\mathbf{U}^H\mathbf{U}=\mathbf{I}$

$= \sigma_z^2 tr(\mathbf{\Sigma^{-2}})$, $tr(\mathbf{\Sigma}^{-2}) = \sum_{i=1}^{k}(1/\sigma_i^2)$, $k=\min(M,N)$ and σ_i is the singular value of $\mathbf{H}$

$$E\{|\hat{\mathbf{Z}}_{ZF}|_2^2\} = \sum_{i=1}^{k}\frac{\sigma_z^2}{\sigma_i^2} \tag{3.5}$$

3.2.2 MMSE signal detection

In order to maximize the post-detection signal-to-interference plus noise ratio (SINR), the MMSE weight matrix is given in Equation (3.6) [12].

$$\mathbf{W}_{MMSE} = (\mathbf{H}^H\mathbf{H} + \sigma_z^2\mathbf{I})^{-1}\mathbf{H}^H \tag{3.6}$$

[2] $|\mathbf{A}|_2$ is the Frobenius norm or the Hilbert–Schmidt norm

[3] tr(A) is the trace of an n-by-n square matrix A, i.e. $tr(A) = a_{11} + a_{22} + \ldots + a_{nn} = \sum_{i=1}^{n} a_{ii}$

Note that the MMSE receiver requires the statistical information of noises, σ_z^2. Using the MMSE weight in Equation (3.6), the following relationship is obtained in Equation (3.7).

$\hat{\mathbf{x}}_{\mathrm{MMSE}} = \mathbf{W}_{\mathrm{MMSE}}\mathbf{y} = (\mathbf{H}^{\mathrm{H}}\mathbf{H}+\boldsymbol{\sigma_z^2}\mathbf{I})^{-1}\mathbf{H}^{\mathrm{H}}\mathbf{y}$, using $\mathbf{y=Hx+z}$

$= (\mathbf{H}^{\mathrm{H}}\mathbf{H}+\sigma_z^2\mathbf{I})^{-1}\mathbf{H}^{\mathrm{H}}\mathbf{Hx} + (\mathbf{H}^{\mathrm{H}}\mathbf{H}+\sigma_z^2\mathbf{I})^{-1}\mathbf{H}^{\mathrm{H}}\mathbf{z}$, let $\tilde{\mathbf{x}} = (\mathbf{I} + \sigma_z^2(\mathbf{H}^{\mathrm{H}}\mathbf{H})^{-1})^{-1}\mathbf{x}$

$$\hat{\mathbf{x}}_{\mathrm{MMSE}} = \tilde{\mathbf{x}} + \tilde{\mathbf{z}}_{\mathrm{MMSE}} \tag{3.7}$$

Where $\tilde{\mathbf{z}}_{\mathrm{MMSE}} = (\mathbf{H}^{\mathrm{H}}\mathbf{H}+\boldsymbol{\sigma_z^2}\mathbf{I})^{-1}\mathbf{H}^{\mathrm{H}}\mathbf{z}$. Using SVD the post-detection noise power is expressed as:

$|\tilde{\mathbf{z}}_{\mathrm{MMSE}}|_2^2 = |(\mathbf{H}^{\mathbf{H}}\mathbf{H} + \sigma_z^2\mathbf{I})^{-1}\mathbf{H}^{\mathbf{H}}\mathbf{z}|^2$

$$|\tilde{\mathbf{z}}_{\mathrm{MMSE}}|_2^2 = |(\mathbf{V}\boldsymbol{\Sigma}^{\mathbf{2}}\mathbf{V}^{\mathbf{H}} + \sigma_z^2\mathbf{I})^{-1}\mathbf{V}\boldsymbol{\Sigma}\mathbf{U}^{\mathbf{H}}\mathbf{z}|^2 \tag{3.8}$$

Because $(\mathbf{V}\boldsymbol{\Sigma}^{\mathbf{2}}\mathbf{V}^{\mathbf{H}} + \sigma_z^2\mathbf{I})^{-1}\mathbf{V}\boldsymbol{\Sigma} = (\mathbf{V}\boldsymbol{\Sigma}^{\mathbf{2}}\mathbf{V}^{\mathbf{H}} + \sigma_z^2\mathbf{I})^{-1}(\boldsymbol{\Sigma}^{-1}\mathbf{V}^{\mathrm{H}})^{-1} = (\boldsymbol{\Sigma}\mathbf{V}^{\mathbf{H}} + \sigma_z^2\boldsymbol{\Sigma}^{-1}\mathbf{V}^{\mathrm{H}})^{-1}$, the noise power in Equation (3.8) can be expressed as:

$$|\tilde{\mathbf{z}}_{\mathrm{MMSE}}|_2^2 = |(\boldsymbol{\Sigma}\mathbf{V}^{\mathrm{H}} + \sigma_z^2\boldsymbol{\Sigma}^{-1}\mathbf{V}^{\mathrm{H}})^{-1}\mathbf{U}^{\mathrm{H}}\mathbf{z}|^2 \quad = |\mathbf{V}(\boldsymbol{\Sigma} + \sigma_z^2\boldsymbol{\Sigma}^{-1})^{-1}\mathbf{U}^{\mathbf{H}}\mathbf{z}|^2 \tag{3.9}$$

Again by the fact that multiplication with a unitary matrix does not change the vector norm, that is, $|\mathbf{Vx}|^2=|\mathbf{x}|^2$, the expected value of Equation (3.9) is given as:

$E\{|\tilde{\mathbf{z}}_{\mathrm{MMSE}}|_2^2\} = E\{|\mathbf{V}(\boldsymbol{\Sigma} + \sigma_z^2\boldsymbol{\Sigma}^{-1})^{-1}\mathbf{U}^{\mathbf{H}}\mathbf{z}|^2\}$

$= E\{\mathrm{tr}((\boldsymbol{\Sigma} + \sigma_z^2\boldsymbol{\Sigma}^{-1})^{-1}\mathbf{U}^{\mathbf{H}}\mathbf{z}\mathbf{z}^{\mathbf{H}}\mathbf{U}(\boldsymbol{\Sigma} + \sigma_z^2\boldsymbol{\Sigma}^{-1})^{-1})\}$

$= \mathrm{tr}((\boldsymbol{\Sigma} + \sigma_z^2\boldsymbol{\Sigma}^{-1})^{-1}\mathbf{U}^{\mathbf{H}}E\{\mathbf{z}\mathbf{z}^{\mathrm{H}}\}\mathbf{U}(\boldsymbol{\Sigma} + \sigma_z^2\boldsymbol{\Sigma}^{-1})^{-1})$

$= \mathrm{tr}(\sigma_z^2(\boldsymbol{\Sigma} + \sigma_z^2\boldsymbol{\Sigma}^{-1})^{-2})$

$= \sum_{i=1}^{k}\sigma_z^2(\sigma_i + \frac{\sigma_z^2}{\sigma_i})^{-2}$

$$E\{|\tilde{\mathbf{z}}_{\mathrm{MMSE}}|_2^2\} = \sum_{i=1}^{k}\frac{\sigma_z^2\sigma_i^2}{(\sigma_i^2+\sigma_z^2)^2} \tag{3.10}$$

Referring to Equations (3.5) and (3.10), the noise enhancement effects due to the minimum singular value for the ZF and MMSE linear detectors are respectively given on Equations (3.11) and (3.12) for $\sigma^2_{min} = \min(\sigma_1^2, \sigma_2^2 \dots \sigma_k^2)$.

$$E\{|\hat{\mathbf{z}}_{ZF}|_2^2\} = \sum_{i=1}^{k} \frac{\sigma_z^2}{\sigma_i^2} \approx \frac{\sigma_z^2}{\sigma_{min}^2} \quad \text{for ZF} \tag{3.11}$$

$$E\{|\tilde{\mathbf{z}}_{MMSE}|_2^2\} = \sum_{i=1}^{k} \frac{\sigma_z^2\sigma_i^2}{(\sigma_i^2+\sigma_z^2)^2} \approx \frac{\sigma_z^2\sigma_{min}^2}{(\sigma_{min}^2+\sigma_z^2)^2} \quad \text{for MMSE} \tag{3.12}$$

Comparing Equation (3.11) to Equation (3.12), it is clear that the effect of noise enhancement in MMSE filtering is less critical than that in ZF filtering. Note that if $\sigma^2_{min} \gg \sigma_z^2$ and thus $\sigma^2_{min} + \sigma_z^2 \approx \sigma^2_{min}$ then the noise enhancement effect of the two linear filters becomes the same.

3.3 Optimum MUD Methods

Let $\mathbf{X}$ is a set of all possible combination of the transmitted signal vectors, $\mathbf{X} = [\mathbf{x}_1, \mathbf{x}_2 \dots \mathbf{x}_L]$, where $\mathbf{x}_i$ is the vector of signals transmitted by each transmitter antenna for i = 1, 2 … L and L is the length of possible combinations. $L=2^{M*B}$, where M is number of transmitting users and B is number of bits per modulated symbol [6].

Optimum detectors are data detectors that make a decision on the transmitted signal in each signal interval based on the observation of the correlation between $\mathbf{y}$ and $\mathbf{H}^*\mathbf{x}_i$ in each interval such that the probability of a correct decision is maximized. The decision rule is based on the computation of the posterior probability given as P(signal $\mathbf{x}_i$ was transmitted | $\mathbf{y}$) = P($\mathbf{x}_i|\mathbf{y}$), i = 1, 2 … L [6].

This criterion maximizes the probability of correct decision and, hence, decreases the probability of error. This decision criterion is called *maximum a posteriori probability* (MAP) criterion. The conditional pdf P($\mathbf{y}|\mathbf{x}_i$) or any monotonic function of it is usually called the likelihood function. The decision criterion based on the maximum of P($\mathbf{y}|\mathbf{x}_i$) over the L signals is called the *maximum likelihood* (ML) criterion. A detector based on the MAP criterion and one that is based on the ML criterion make the same decision as long as the a priori probabilities P($\mathbf{x}_i$) are all equal [6].

3.3.1 ML detection

Maximum likelihood detection calculates the Euclidean distance between the received signal vector, **y**, and the product of all possible transmitted signal vectors, **x**, with the given channel **H**, and finds the one with the minimum distance. Let **C** and M denote a set of signal constellation symbol points and a number of transmit antennas, respectively. Then, ML detection determines the estimate of the transmitted signal vector **x** as [6]:

$$\hat{\mathbf{x}}_{\mathrm{ML}} = arg_{\boldsymbol{x}\epsilon C^M}^{min} |\boldsymbol{y} - \boldsymbol{H}\boldsymbol{x}|^2 \tag{3.13}$$

Where $|\mathbf{y} - \mathbf{Hx}|^2$ corresponds to the ML metric (equivalent to log likelihood function). The ML method achieves the optimal performance as the maximum aposteriori probability (MAP) detection when all the transmitted vectors are equally likely. However, its complexity increases exponentially as modulation order and/or the number of transmit antennas increases.

The required number of ML metric calculation is C^M, that is, the complexity of metric calculation exponentially increases with the number of antennas. Even if this particular method suffers from computational complexity, its performance serves as a reference to other detection methods since it corresponds to the best possible performance [6].

3.3.2 Sphere detection

Although the worst-case complexity of the ML search increases exponentially with M, the average complexity may be much less. An example of a search algorithm with relatively low average complexity, assuming the Gaussian noise model, is the sphere decoder [12, 15].

To describe the sphere decoder, first observe that if each component of **x** is selected from a rectangular constellation, then each **x** corresponds to a point in a rectangular lattice. The ML estimate can then be computed by performing an exhaustive search over that lattice. To reduce the search complexity, the sphere decoder restricts **x** to lie in a hyper sphere of radius r centered at **y**. If the hyper sphere contains at least one lattice point, then this restricted search still gives the ML estimate [15].

3.4 SIC signal detection

In general, the performance of the linear detection methods is worse than that of other nonlinear receiver techniques. However, linear detection methods require a low complexity of hardware implementation. It is possible to improve their performance without increasing the complexity significantly by an ordered successive interference cancellation (OSIC) method.

It is a bank of linear receivers, each of which detects one of the parallel data streams, with the detected signal components successively canceled from the received signal at each stage. More specifically, the detected signal in each stage is subtracted from the received signal so that the remaining signal with the reduced interference can be used in the subsequent stage [12].

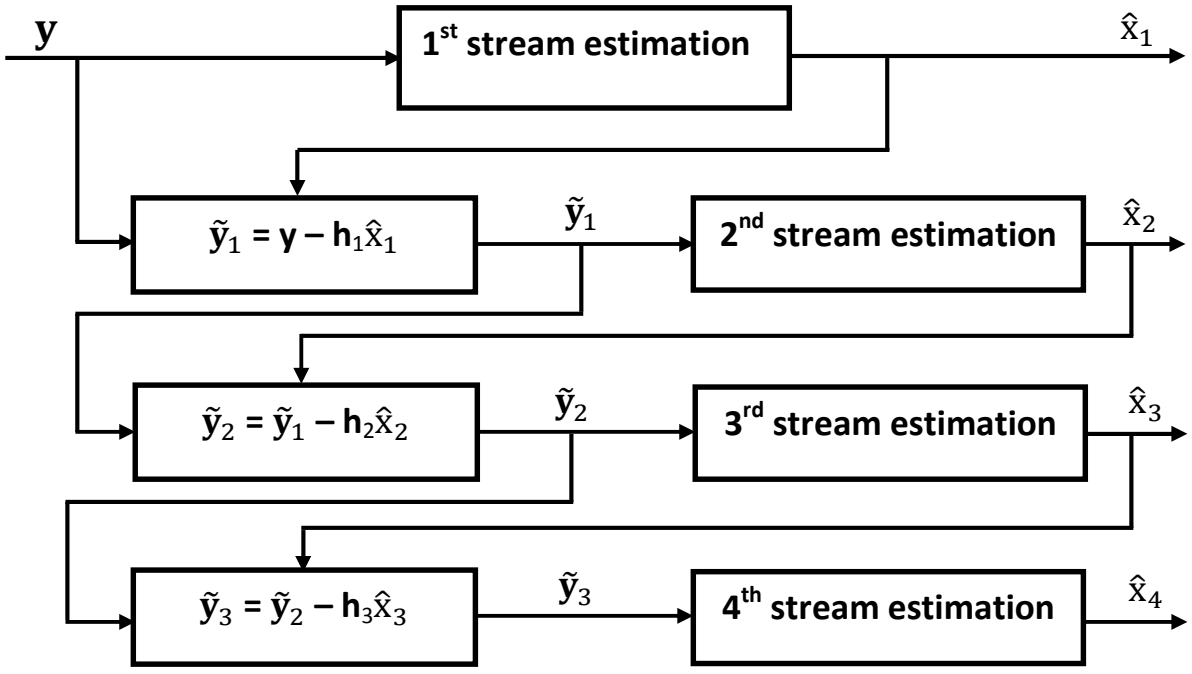

Figure 7: OSIC signal detection for four spatial streams.

CHAPTER 4

GENETIC ALGORITHM

4.1 Introduction

The Industrial Revolution, which started in England around 1760, has replaced human muscle power with the machine. Artificial intelligence (AI) aims at replacing human intelligence with the machine. The work on artificial intelligence started in the early 1950s, and the term itself was coined in 1956. The Webster's new world college dictionary, third edition describes AI as [19]:

Definition 3: Artificial intelligence

Artificial intelligence is the capability of computers or programs to operate in ways to mimic human thought processes, such as reasoning and learning.

The second characterization of intelligent computation is based on the underlying mechanism for biological processes used to arrive at a solution. The primary examples of this category are neural networks and evolutionary computations.

Evolutionary computation techniques abstract evolutionary principles into algorithms that may be used to search for optimal solutions to a problem. In a search algorithm, a number of possible solutions to a problem are available and the task is to find the best solution possible in a fixed amount of time [20].

Definition 4: Evolutionary algorithm

An evolutionary algorithm (EA) is an iterative and stochastic process that operates on a set of individuals and each individual represents a potential solution to the problem being solved.

Some of evolutional methods include the genetic algorithm (Holland, 1975), simulated annealing (Kirkpatrick et al., 1983), particle swarm optimization

(Parsopoulos and Vrahatis, 2002), ant colony optimization (Dorigo and Maria, 1997), and evolutionary algorithms (Schwefel, 1995). These methods generate new points in the search space by applying operators to current points and statistically moving toward more optimal places in the search space [17].

Definition 5: Genetic algorithm

Genetic algorithm (GA) is an optimization and search technique based on the principles of genetics and natural selection. GA allows a population composed of many individuals to evolve under specified selection rules to a state that minimizes the cost function [18].

Through these processes, genetic algorithms find better and better solutions to a problem just as species evolve to better adapt to their environments. Genetic algorithms have been extended in their ways of representing solutions and performing basic processes [19].

Optimization is the process of adjusting the inputs to or characteristics of a device, mathematical process, or experiment to find the minimum or maximum output or result. The input consists of variables; the process or function to be optimized is known as the cost function, objective function, or fitness function; and the output is the cost or fitness [18].

Definition 6: Mathematical optimization

In mathematics or computer science mathematical optimization (alternatively, optimization or mathematical programming) is the selection of a best element (with regard to some criteria) from some set of available alternatives.

Definition 7: Optimization problem

An optimization problem can be represented in the following way; Given: a function f from some set A to the real numbers, Sought: an element x_0 in A such that $f(x_0) \leq f(x)$ for all x in A ("minimization") or such that $f(x_0) \geq f(x)$ for all x in A ("maximization").

4.2 Terminologies

Definition 8: Search space

The space of all feasible solutions (the set of solutions among which the desired solution resides) is called search space (also called state space).

Each and every point in the search space represents one possible solution. Therefore, each possible solution can be marked by its fitness value depending on the problem definition.

The two distinct elements in GA are individuals and populations. An individual is a single solution while the population is the set of individuals currently involved in the search process. Individual groups together two forms of solutions the chromosome, which is the raw 'genetic' information (*genotype*) that the GA deals and the *phenotype*, which is the expressive of the chromosome in the terms of the model [17].

Definition 9: Chromosome

A chromosome is an organized structure of DNA, protein, and RNA found in cells. It is a single piece of coiled DNA containing many genes, regulatory elements and other nucleotide sequences.

For the sake of simplification, in genetic algorithms the term chromosome refers to a solution candidate. It is remarkable that most applications of genetic algorithms employ haploid, single chromosome individuals.

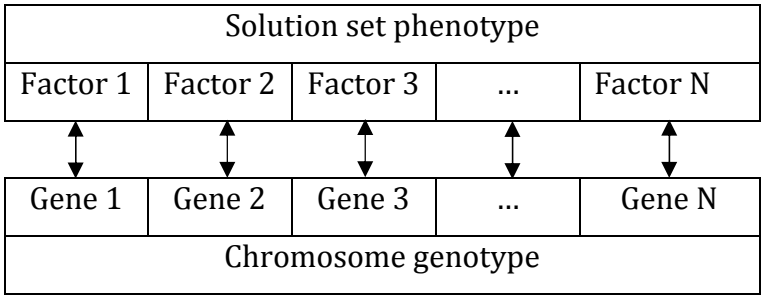

Figure 8: Representation of genotype and phenotype.

A chromosome is subdivided into genes. Gene is the GA's representation of a single factor for a control factor. Each factor in the solution set corresponds to gene in the chromosome. Figure 8 shows the representation of a genotype.

1 1 0 1 0 0 0 1 0 1 1 0 0 1 0 1

Figure 9: Representation of a chromosome.

Genes are the basic "instructions" for building genetic algorithms. The structure of each gene is defined in a record of phenotyping parameters. The phenotype parameters are instructions for mapping between genotype and phenotype. It can also be said as encoding a solution set into a chromosome and decoding a chromosome to a solution set.

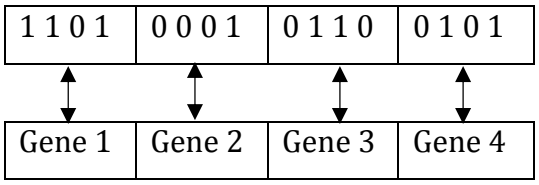

Figure 10: Representation of a gene.

A population is a collection of individuals. A population consists of a number of individuals being tested, the phenotype parameters defining the individuals and some information about search space. The two important aspects of population used in genetic algorithms are: the initial population and the population size.

Population	Chromosome 1	1 1 0 0 1 0 0 0 1 0 1 1 1 1 0 0
	Chromosome 2	0 0 0 1 1 0 1 1 1 0 0 1 0 1 0 1
	Chromosome 3	0 1 0 1 0 1 0 0 0 1 1 0 1 1 1 1
	Chromosome 4	1 0 1 0 1 1 1 1 0 0 1 0 0 1 0 1

Table 1: Population

For each and every problem, the population size will depend on the complexity of the problem. Often a random initialization of population is carried. In the case of a

binary coded chromosome this means, that each bit is initialized to a random zero or one. But there may be instances where the initialization of population is carried out with some known good solutions.

Ideally, the first population should have a gene pool as large as possible in order to be able to explore the whole search space. To achieve this, the initial population is, in most of the cases, chosen randomly. A large population is quite useful. But it requires much more computational cost, memory, and time [17].

The fitness of an individual in a genetic algorithm is the value of an objective function for its phenotype. For calculating fitness, the chromosome has to be first decoded and the objective function has to be evaluated. The fitness not only indicates how good the solution is, but also corresponds to how close the chromosome is to the optimal one. In the case of a minimization problem, the fittest individuals will have the lowest numerical value of the associated objective function.

Encoding is a process of representing individual genes. The process can be performed using bits, numbers, trees, arrays, lists or any other objects. The encoding depends mainly on solving the problem [17].

a. Binary encoding: The most common way of encoding is a binary string, which would be represented as in Table 2. Each chromosome encodes a binary string. Binary encoding gives many possible chromosomes with a smaller number of alleles.

Chromosome 1	1 1 0 0 1 0 0 0 1 0 1 1 1 1 0 0
Chromosome 2	0 0 0 1 1 0 1 1 1 0 0 1 0 1 0 1

Table 2: Binary encoding

b. Octal encoding: This encoding uses string made up of octal numbers (0–7). Table 3 gives an example of octal encoded chromosomes.

Chromosome 1	67545213
Chromosome 2	05467412

Table 3: Octal encoding

c. Hexadecimal encoding: Hexadecimal encoding uses string made up of hexadecimal numbers (0–9, A–F). Two examples of octal encoding are given on Table 4.

Chromosome 1	95624A1C
Chromosome 2	F48960EB

Table 4: Hexadecimal encoding

d. Value encoding: Direct value encoding can be used in problems, where some complicated values, such as real numbers or complex numbers, are used. Use of binary encoding for this type of problems would be very difficult.

Chromosome A	4.6587 1.0258 7.3356 0.4751
Chromosome B	1+2i 4-9i 5i 9+7i
Chromosome C	Back right forward left

Table 5: Value encoding

4.3 GA Operators

The breeding process is the heart of the genetic algorithm. It is in this process, the search process creates new and hopefully fitter individuals. The breeding cycle consists of four steps: selection, crossover, mutation and replacement operations [17].

Step 1: Selecting parents - *Selection*.

Step 2: Crossing the parents to create new individuals (children) - *Crossover*.

Step 3: Introducing new genetic structures in the population – *Mutation*.

Step 4: Replacing old individuals in the population with the new ones - *Replacement*.

4.3.1 Selection

Selection is the process of choosing two parents from the population for crossing. After deciding on an encoding, the next step is to decide how to perform selection i.e., how to choose individuals in the population that will create offspring for the next generation and how many offspring each will create. The purpose of selection is to emphasize fitter individuals in the population in hopes that their offsprings have higher fitness.

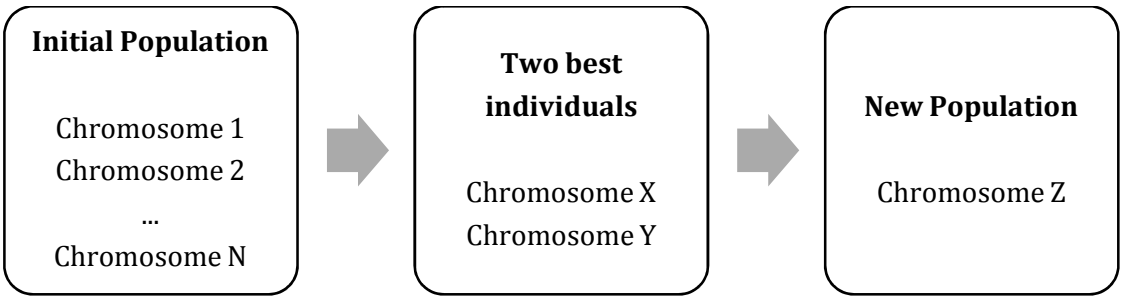

Figure 11: Selection

The convergence rate of GA is largely determined by the magnitude of the selection pressure. In addition to providing selection pressure, selection schemes should also preserve population diversity, as this helps to avoid premature convergence. The various selection methods are discussed as follows [17].

a. Roulette wheel selection: The principle of roulette wheel selection is a linear search through a roulette wheel with the slots in the wheel weighted in proportion to the individual's fitness values.

b. Random selection: This technique randomly selects a parent from the population. In terms of disruption of genetic codes, random selection is more disruptive, on average, than roulette wheel selection.

c. Rank selection: Rank Selection selects the individuals based on their fitness values. It keeps up selection pressure when the fitness variance is low. In effect, potential parents

are selected and a tournament is held to decide which of the individuals will be the parent.

d. Tournament selection: An ideal selection strategy should be such that it is able to adjust its selective pressure and population diversity so as to fine-tune GA search performance.

4.3.2 Crossover

After the selection process, the population is enriched with better individuals. Crossover operator is applied to the mating pool with the hope that it creates a better offspring. Crossover is the process of taking two parent solutions and producing from them a child [17].

a. Single point crossover: The canonical genetic algorithm uses single point crossover, where the two mating chromosomes are cut once at corresponding points and the sections after the cuts exchanged. The crossover point is selected randomly along the length of the mated strings and bits next to the cross-sites are exchanged.
b. Two point crossover: In two-point crossover, two crossover points are chosen randomly and the contents between these points are exchanged between two mated parents.
c. Multi-point crossover: For multi-point crossover, *m* crossover positions are chosen at random with no duplicates and sorted into ascending order. Then, the bits between successive crossover points are exchanged between the two parents to produce two new offspring. The section between the first allele position and the first crossover point is not exchanged between individuals. This process is illustrated in Figure 12-c for *m*=5.
d. Uniform crossover: Uniform crossover is quite different from the N-point crossover. Each gene in the offspring is created by copying the corresponding gene from one or the other parent chosen according to a random generated binary crossover mask of the same length as the chromosomes.

Parent 1	1 1 0 1 0 0 1 1 0 1
Parent 2	0 1 0 0 1 1 0 1 0 0
Child 1	1 1 0 1 0 0 0 1 0 0
Child 2	0 1 0 0 1 1 1 1 0 1

a) Single point crossover

Parent 1	1 1 0 1 0 0 1 1 0 1
Parent 2	0 1 0 0 1 1 0 1 0 0
Child 1	1 1 0 1 1 1 0 1 0 1
Child 2	0 1 0 0 0 0 1 1 0 0

b) Two point crossover

Parent 1	1 1 0 1 0 0 1 1 0 1 0 0 1 0 0
Parent 2	0 1 0 0 1 1 0 1 0 0 1 0 1 0 0 1 0 1 1
Child 1	1 1 0 0 1 0 1 1 0 0 1 0 1 0 1 1 0 0 1 1
Child 2	0 1 0 1 0 1 0 1 0 1 0 0 1 0 0 0 1 1 0 0

c) Multi-point crossover

Parent 1	1 0 1 1 0 0 1 1
Parent 2	0 0 0 1 1 0 1 0
Mask	1 1 0 1 0 1 1 0
Child 1	1 0 0 1 1 0 1 0
Child 2	0 0 1 1 0 0 1 1

d) Uniform crossover

Figure 12: Crossover techniques

4.3.3 Mutation

Mutation is viewed as a background operator to maintain genetic diversity in the population. It introduces new genetic structures in the population by randomly modifying some of its building blocks. Mutation helps escape from local minima's trap and maintains diversity in the population. Some of the methods are described below [17].

a. Flipping: Flipping of a bit involves changing 0 to 1 and 1 to 0 based on a mutation chromosome generated. Table 6 explains mutation-flipping concept.

Parent	1 0 1 0 1 1 1 0
Mutation chromosome	0 1 1 0 1 0 0 0
Child	1 1 0 0 0 1 1 0

Table 6: Flipping

b. Interchanging: Two random positions of the string are chosen and the bits corresponding to those positions are interchanged. This is shown in Table 7.

Parent	1 **0** 1 0 1 **1** 1 0
Child	1 **1** 1 0 1 **0** 1 0

Table 7: Interchanging

c. Reversing: A random position is chosen and the bits next to that position are reversed and child chromosome is produced. This is shown in Table 8.

Parent	1 0 1 0 1 1 **1 0**
Child	1 0 1 0 1 1 **0 1**

Table 8: Reversing

The important parameter in the mutation technique is the *mutation probability* (Pm). The mutation probability decides how often parts of chromosome will be mutated.

4.3.4 Replacement

Replacement is the last stage of any breeding cycle. It is a technique used to decide which individual stay in a population and which is replaced in a parent population [17].

a. Random replacement: The two children replace two randomly chosen individuals in the population.
b. Weak parent replacement: The weaker parent is replaced by a strong child. With the four individuals only the fittest two, parent or child, return to population.
c. Both parents replacement: The child replaces the parent. In this case, each individual only gets to breed once.
d. Tournament replacement: Competitions are run between sets of individuals from the last and the actual generation, with the winners becoming part of the new population.

CHAPTER 5

SYSTEM DESIGN

5.1 System Model

As shown in Figure 13, system under study is for an uplink communication system with four users at the mobile station. Each mobile user has independent data source, channel encoder, modulator, and transmitter antenna. The users transmit their signal at the same frequency band and at the same time slot using the principle of MU-MIMO. At the basestation there are two receiver antennas which are separated by $\lambda/2$ minimum distance, CE and MUD module, channel decoder, and final destination.

Each user's digital data stream, $\mathbf{b_i}$ i=1, 2, 3, and 4, is used to represent the information to be communicated to the destination. Sequences of the i^{th} user binary digits (bits) are called information sequence $\mathbf{b_i}$. The channel encoder transforms the information sequence $\mathbf{b_i}$ into a discrete encoded sequence $\mathbf{b_i^c}$ called a codeword. The channel encoder used is low-density parity-check encoder due to its amenability to high coding rate, lower error floor, and superior burst error correcting capability [66]. The code rate of the LDPC encoder is ¼.

The encoded data $\mathbf{b_i^c}$ is then modulated by the modulator block using 16-ary quadrature amplitude modulation (QAM). The constellation diagram of 16-QAM is given in Figure 14. The constellation consists of a square lattice of signal points. The general form of QAM signal can be defined on Equation (5.1) [3].

$$S_i(t) = \sqrt{\frac{2E_{min}}{T_s}}[a_i\cos(2\pi f_c t) - b_i\sin(2\pi f_c t)] \quad (5.1)$$

For $0 \le t \le T_s$ and i=1, 2 … 16. E_{min} is energy of the signal with the lowest amplitude and a_i and b_i, (a_i, b_i), is a pair of independent integers chosen according to the location of a particular signal point.

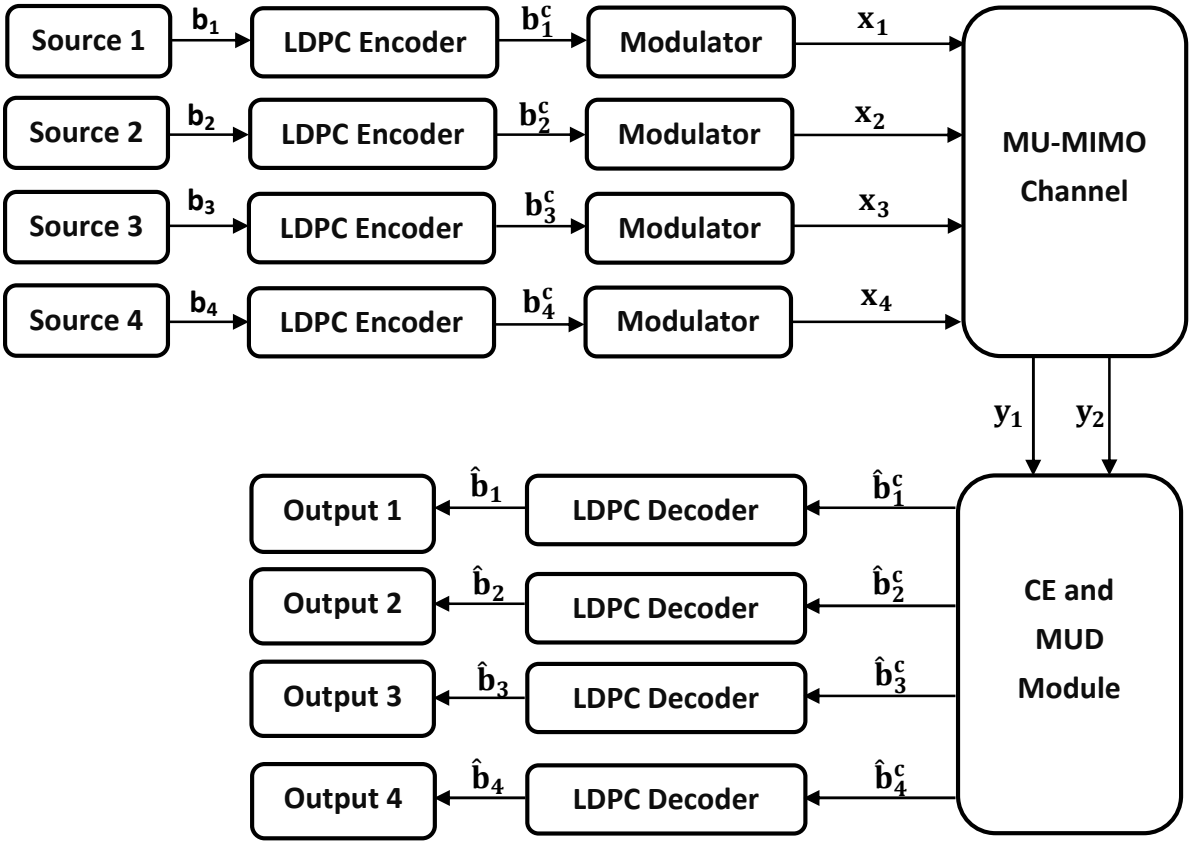

Figure 13: Uplink communication system schematic diagram.

The signal $S_i(t)$ can be expanded in terms of a pair basis functions defined in Equation (5.2):

$$\Phi_1(t) = \sqrt{\frac{2}{T_s}}\cos(2\pi f_c t) \quad \text{and} \quad \Phi_2(t) = -\sqrt{\frac{2}{T_s}}\sin(2\pi f_c t), \quad 0 \le t \le T_s \tag{5.2}$$

The coordinates of the i^{th} message point are $a_i\sqrt{E_{min}}$ and $b_i\sqrt{E_{min}}$ where (a_i, b_i) is an element of the 4x4 matrix given below.

$$(a_i, b_i) = \begin{bmatrix} (-3, 3) & (-1, 3) & (1, 3) & (3, 3) \\ (-3, 1) & (-1, 1) & (1, 1) & (3, 1) \\ (-3, -1) & (-1, -1) & (1, -1) & (3, -1) \\ (-3, -3) & (-1, -3) & (1, -3) & (3, -3) \end{bmatrix} \tag{5.3}$$

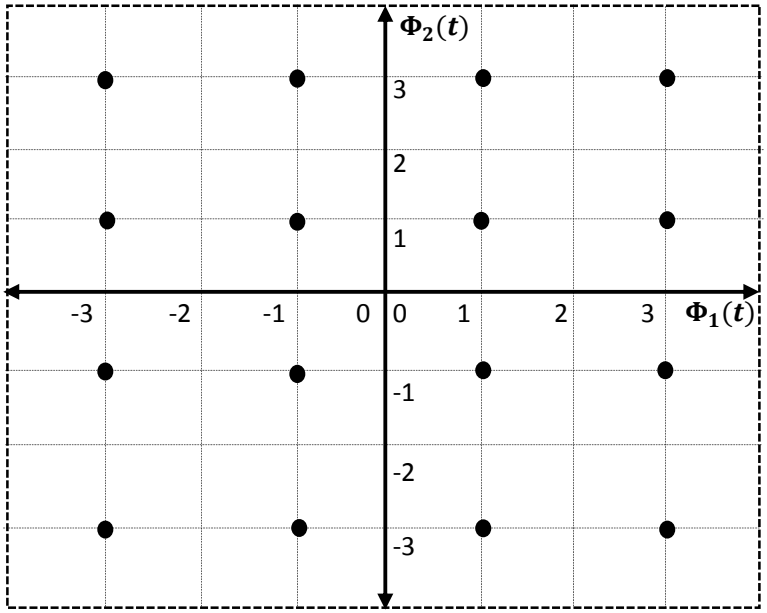

Figure 14: Constellation diagram of 16-QAM signal set.

The complex baseband representation of the bandpass signal $S_i(t)$ is given in Equation (5.4).

$$g_i = \sqrt{\frac{2E_{min}}{T_s}}(a_i + jb_i),\ i=1, 2 \dots 16 \tag{5.4}$$

The output of each modulator is represented by a complex envelope of baseband signal x_i, where $x_i \in G$ for i=1, 2, 3, and 4 and G is the set of complex baseband elements, i.e. $G = \{g_1, g_2 \dots g_{16}\}$. These signals, i.e. $\mathbf{x} = [x_1; x_2; x_3; x_4]$, are transmitted by the transmitter antennas and used as an input to the MU-MIMO channel. The transmission power of the signal x_i is $Ps=P_{min}* (a_i^2 + b_i^2)$ where $P_{min}=\frac{E_{min}}{T_s}$.

The MU-MIMO transmission channel **H**, which is given on Equation (2.2), is used here for M=4 and N=2 and the representation is shown on Equation (5.5).

$$\mathbf{H} = \begin{bmatrix} h_{11} & h_{12} & h_{13} & h_{14} \\ h_{21} & h_{22} & h_{23} & h_{24} \end{bmatrix} \tag{5.5}$$

Each elements of matrix **H**, h_{ij} for i=1 and 2 and j=1, 2, 3, and 4, is used to represent the path from transmitter antenna j to receiver antenna i. The path h_{ij} is equivalently represented by $h_{ij} = c_{ij} + j*d_{ij}$ where c_{ij} and d_{ij} are normally distributed random variables with mean 0 and standard deviation $\sqrt{2}/2$.

In addition to fading due to the channel characteristics there is addition of white gaussian noise at the receiver. Average power of the noise signal is represented by P_n. The resulting signals received by the receiver antennas, i.e. y_1 and y_2, are described by Figure 15 and Equation (5.6).

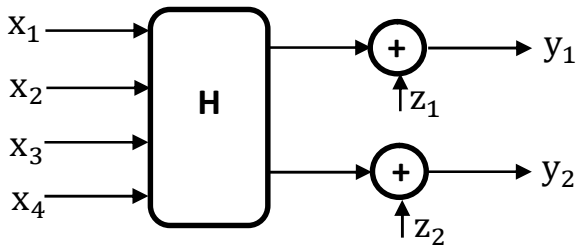

Figure 15: System model of the transmission channel.

$$\mathbf{y} = \mathbf{Hx} + \mathbf{z} \tag{5.6}$$

Where **y** is the received signal vector, **H** is the channel transfer function matrix, and **z** is the AWGN vector. The expanded representation of Equation (5.6) is:

$$\begin{bmatrix} y_1 \\ y_2 \end{bmatrix} = \begin{bmatrix} h_{11} & h_{12} & h_{13} & h_{14} \\ h_{21} & h_{22} & h_{23} & h_{24} \end{bmatrix} \begin{bmatrix} x_1 \\ x_2 \\ x_3 \\ x_4 \end{bmatrix} + \begin{bmatrix} z_1 \\ z_2 \end{bmatrix} \tag{5.7}$$

The symbols y_1 and y_2 are used to represent received signals at the receiver antennas and used as an input for receiver device. The receiver device first estimates the CTF matrix **H** using CE block and then the MUD block estimates the transmitted data signals $\hat{\mathbf{b}}_\mathbf{i}^\mathbf{c}$ using the estimated FD-CTF matrix $\widehat{\mathbf{H}}$ and the received user data signal **y**. Both blocks use GA to estimate the required parameters. Finally LDPC based channel decoder decodes the estimated sequences of bits and gives the transmitted user data bit estimates, $\hat{\mathbf{b}}_\mathbf{i}$ for i=1, 2, 3, and 4.

5.2 CE Algorithm

5.2.1 Pilot signal structure

The transmitted baseband signal block structure, **X**, that consists of the pilot signals, used for channel estimation, and the main user data signals, which used to carry user information, can be represented by Equation (5.8).

$$\mathbf{X} = \left[\mathbf{x_{p1}^1} \quad \dots \quad \mathbf{x_{pm}^1} \quad \mathbf{x_{d1}^1} \quad \mathbf{x_{d2}^1} \quad \dots \quad \mathbf{x_{dn}^1} \quad \mathbf{x_{p1}^2} \quad \dots \quad \mathbf{x_{pm}^2} \quad \mathbf{x_{d1}^2} \quad \mathbf{x_{d2}^2} \quad \dots \quad \mathbf{x_{dn}^2} \quad \dots\right] \quad (5.8)$$

Where $\mathbf{x_{pi}^k}$ refers the ith pilot signal vector for i=1, 2… m and $\mathbf{x_{dj}^k}$ refers to the jth user data signal vector for j=1, 2 … n. These modulated data signals are then transmitted and the equivalent received signal block resulting from Equation (5.6) will be:

$$\mathbf{Y} = \left[\mathbf{y_{p1}^1} \quad \dots \quad \mathbf{y_{pm}^1} \quad \mathbf{y_{d1}^1} \quad \mathbf{y_{d2}^1} \quad \dots \quad \mathbf{y_{dn}^1} \quad \mathbf{y_{p1}^2} \quad \dots \quad \mathbf{y_{pm}^2} \quad \mathbf{y_{d1}^2} \quad \mathbf{y_{d2}^2} \quad \dots \quad \mathbf{y_{dn}^2} \quad \dots\right] \quad (5.9)$$

Where $\mathbf{y_{pi}^k}$ represents the ith received pilot signal vector for i=1… m and $\mathbf{y_{dj}^k}$ is the jth received user data vector for j=1, 2 … n at the kth frame. The values of m and n, i.e. the number of pilot and data signals per frame, depend on the nature of the communication channel, the number of transmitter and receiver antennas, and the value of accuracy required at the receiver device.

The pilot signals are mainly used to estimate the channel transfer function matrix **H** and they are known both at the transmitter and the receiver. Using 4 pilot signals per transmitter antenna the resulting received pilot signals at the receiver looks on Equations (5.10) and (5.11).

$$\begin{bmatrix} y_{p11} & y_{p12} & y_{p13} & y_{p14} \\ y_{p21} & y_{p22} & y_{p23} & y_{p24} \end{bmatrix} = \begin{bmatrix} h_{11} & h_{12} & h_{13} & h_{14} \\ h_{21} & h_{22} & h_{23} & h_{24} \end{bmatrix} \begin{bmatrix} x_{p11} & x_{p12} & x_{p13} & x_{p14} \\ x_{p21} & x_{p22} & x_{p23} & x_{p24} \\ x_{p31} & x_{p32} & x_{p33} & x_{p34} \\ x_{p41} & x_{p42} & x_{p43} & x_{p44} \end{bmatrix} + \begin{bmatrix} z_{11} & z_{12} & z_{13} & z_{14} \\ z_{21} & z_{22} & z_{23} & z_{24} \end{bmatrix} \quad (5.10)$$

$$\mathbf{Y}_p = \mathbf{H}\mathbf{X}_p + \mathbf{Z} \quad (5.11)$$

5.2.2 Proposed GA-based CE

The proposed GA-based channel estimator is used to estimate FDCTF matrix **H** based on the transmitted pilot signals, $\mathbf{X}_p$, and the received pilot signals, $\mathbf{Y}_p$. GA-based channel estimator algorithm consists of the initialization, selection, crossover, mutation, and replacement operators. The flow chart and pseudocode for complex number based genetic algorithm is given below.

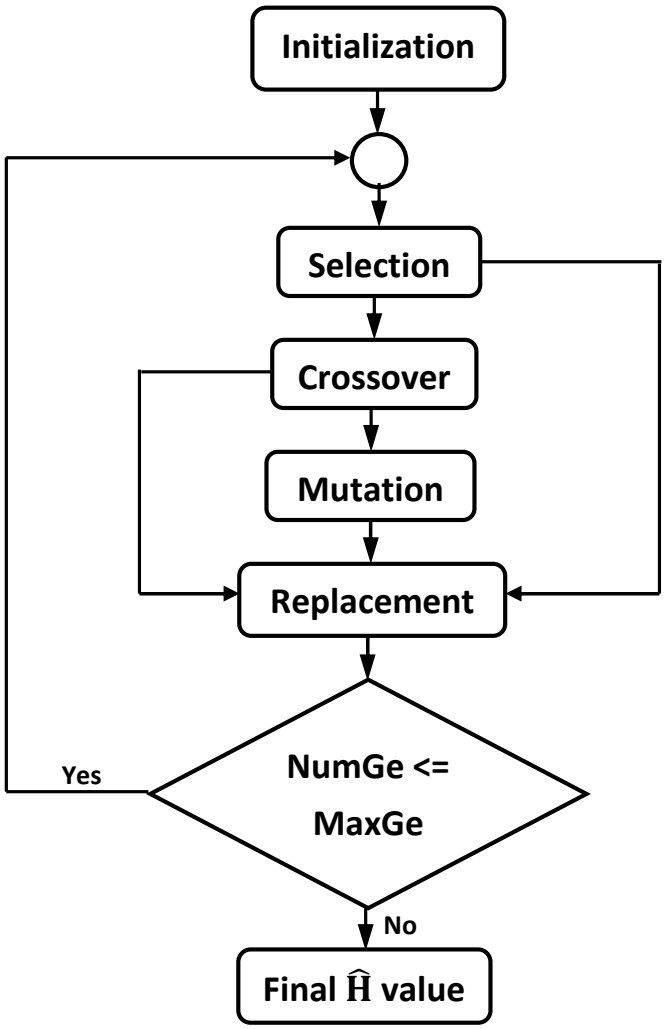

Figure 16: Flow chart of GA-based channel estimator.

The following parameters are used in GA-based CE algorithm:

- Xp – number of individuals in a generation.
- Xn – number of individuals per tournament group.
- Xpp – total number of selected individuals, Xpp = Xrt*Xp.
- Xrt – ratio of selected individuals per total population, constant.
- Yg – number of generations.
- Y_{Tot} – total number of generations, i.e. $Y_{Tot} = Yg + 1$.
- Xr – replacement convergence size.
- Xp' – number of individuals selected for next generation, Xp' = Xp – Xr.

The pseudocode for GA-based CE algorithm is given below and each operation in the algorithm will be discussed in details on the following topics.

Proposed GA-based CE algorithm

1. **Start GACE**
2. **Initialize H** with Xp elements
3. **For** i = 1: Yg
4. **Select** Xpp individuals
5. **Crossover** to each other
6. **Mutate** the result of Step 5
7. **Replace** week parents with better children
8. **End For**
9. $\widehat{\mathbf{H}} = \mathbf{H}$ga
10. **End GACE**

5.2.2.1 Initialization

There are two methods to initialize the first generation of GA-based channel estimator. The first method is to initialize using random number generators called *random initialization method*. This method is the easiest one but the algorithm requires longer time to converge to the solution. The second method is to initialize using a first individual obtained by other CE methods listed in Chapter 2 and then increase the number of individuals using mutation operation.

The number of individuals in the initialization stage determines the accuracy of the algorithm, time required to finish the estimation, and complexity. As the number of initial population increases, the probability that the result put in a local minima decreases and computational complexity increases.

For the system modeled above random initialization is used to generate the populations of the first generation. There are Xp individuals that are generated randomly using the same statistical properties as the channel behavior. The set of individuals in the first generation is: $\mathbf{H}_0 = [\mathbf{H}_{01}, \mathbf{H}_{02} \ldots \mathbf{H}_{0Xp}]$, where $\mathbf{H}_{ij}$ represents the j^{th} individual in i^{th} generation.

5.2.2.2 Selection

The next step after the initialization or the replacement operation is selection operation, as seen on Figure 16. Different selection methods are listed in Chapter 4. Roulette Wheel, tournament, and rank selection methods are among the most widely used ones. For this system *tournament selection* is used and it divides the whole population in to groups and selects the best individuals among each group.

The best individuals in the generation are selected based on their fitness value. Fitness values of all the individuals are calculated from the cost function given in Equation (5.12).

$$\text{Cost Function} = |\mathbf{Y_p} - \mathbf{H_{est}} * \mathbf{X_p}|^2 \qquad (5.12)$$

Tournament selection has large convergence strength and has good ability for diversity. The advantage here is that it requires less time to converge and divides the whole population in group to form diversity. The pseudocode is given below.

GA-based CE selection algorithm

1. **Start Selection**

2. **Input** $\mathbf{H}_i$, **Y**p and **X**p

3. **For** j = 1: Xp

4. FitVal (j) = $|\mathbf{Y}p - \mathbf{H}_{ij}\mathbf{X}p|^2$

5. **End For**

6. **Initialize** Xn and Xrt

7. **Divide** the population in groups of Xn individuals

8. **For** k=1: Xp/Xn

9. **For** l=1: Xrt*Xn

10. [a, b] = **min** (FitVal ((k-1)*Xn+1: k*Xn))

11. $\mathbf{H}^p_{i((k-1)*Xrt*Xn+l)} = \mathbf{H}_{i((k-1)*Xn+b)}$

12. FitVal ((k-1)*Xn+b) = 1000

13. **End For**

14. **End For**

15. **Output** $\mathbf{H}_i^p$

16. **End Selection**

From selection operation Xpp = Xrt*Xp individuals are obtained and the result is given on Equation (5.13).

$$\mathbf{H}_i^p = [\mathbf{H}_{i1}^p, \mathbf{H}_{i2}^p \ \dots \ \mathbf{H}_{iXpp}^p] \tag{5.13}$$

5.2.2.3 Crossover

The selection stage gives relatively the fittest individuals per tournament groups. These selected individuals are used as an input for the breading process, i.e. crossover. The crossover operator produces children from the selected parents by combining individual gens together or by taking the average values of genes.

Let the parent individuals are $\mathbf{H}_{ij}^{p}$ and $\mathbf{H}_{ij+1}^{p}$ for j=1, 3 … Xpp-1 from Equation (5.13) and represented on Equation (5.14). By using one point and uniform crossover it is possible to generate the children $\mathbf{H}_{ij}^{c1}$, $\mathbf{H}_{ij}^{c2}$ and $\mathbf{H}_{ij}^{c3}$ from Equation (5.15) and (5.16).

$$\mathbf{H}_{ij}^{p} = \begin{bmatrix} h_{11} & h_{12} & h_{13} & h_{14} \\ h_{21} & h_{22} & h_{23} & h_{24} \end{bmatrix} \quad \text{and} \quad \mathbf{H}_{ij+1}^{p} = \begin{bmatrix} h'_{11} & h'_{12} & h'_{13} & h'_{14} \\ h'_{21} & h'_{22} & h'_{23} & h'_{24} \end{bmatrix} \tag{5.14}$$

$$\mathbf{H}_{ij}^{c1} = \begin{bmatrix} h_{11} & h_{12} & h_{13} & h_{14} \\ h'_{21} & h'_{22} & h'_{23} & h'_{24} \end{bmatrix} \quad \text{and} \quad \mathbf{H}_{ij}^{c2} = \begin{bmatrix} h'_{11} & h'_{12} & h'_{13} & h'_{14} \\ h_{21} & h_{22} & h_{23} & h_{24} \end{bmatrix} \tag{5.15}$$

$$\mathbf{H}_{ij}^{c3} = (\mathbf{H}_{ij}^{p} + \mathbf{H}_{ij+1}^{p})/2 \tag{5.16}$$

For Xpp=Xrt*Xp selected parents, there are 1.5*Xpp children are obtained by using crossover operation.

$$\mathbf{H}_{i}^{c} = [\mathbf{H}_{i1}^{c}, \mathbf{H}_{i2}^{c} \ldots \mathbf{H}_{i1.5*Xpp}^{c}] \tag{5.17}$$

5.2.2.4 Mutation

As mentioned in Chapter 4 mutation prevents the algorithm to be trapped in a local minimum. Mutation plays the role of recovering the lost genetic materials as well as for randomly disturbing genetic information. Uniform mutation is used for GA-based CE algorithm. The output of the crossover operation, i.e. the children $\mathbf{H}_{ij}^{c}$ in the i^{th} generation and for j=1, 2 … 1.5*Xpp, used as an input for the mutation step.

There are M*N=4*2=8 genes per individual and each gene has a real and an imaginary part 2*M*N=16, therefore the mutation probability is 1/16.

GA-based CE mutation operation

1. **Start Mutation**
2. **Input** $\mathbf{H}_i^c$
3. **Initialize** $\mathbf{H}_i^m$
4. **For** k=1: 1.5*Xpp
5. **For** l=1: N*M
6. **Select** the l^{th} gene of the k^{th} child h_l^{ck}
7. $Temp_1$ = real (h_l^{ck}) + lmax
8. $Temp_2$ = real (h_l^{ck}) - lmax
9. $Temp_3$ = imag (h_l^{ck}) + lmax
10. $Temp_4$ = imag (h_l^{ck}) - lmax
11. $h_l^{m[(k-1)*32+(l-1)*4+1]}$ = complex ($Temp_1$, imag (h_l^{ck}))
12. $h_l^{m[(k-1)*32+(l-1)*4+2]}$ = complex ($Temp_2$, imag (h_l^{ck}))
13. $h_l^{m[(k-1)*32+(l-1)*4+3]}$ = complex (real (h_l^{ck}), $Temp_3$)
14. $h_l^{m[(k-1)*32+(l-1)*4+4]}$ = complex (real (h_l^{ck}), $Temp_4$)
15. **End For**
16. **End For**
17. **Output** $\mathbf{H}_i^m$
18. **End Mutation**

The value of the mutation step size, lmax, depends on the variation of the CTF. There are 4*M*N*1.5*Xpp = 48*Xpp children obtained from the mutation operation.

$$\mathbf{H}_i^m = [\mathbf{H}_{i1}^m, \mathbf{H}_{i2}^m \ldots \mathbf{H}_{i48*Xpp}^m] \quad (5.18)$$

5.2.2.5 Replacement

The selection method used in the replacement stage is rank selection. The Xpp parents and 49.5*Xpp children are combined and gives 50.1*Xpp individuals for selection. Rank selection method selects Xp' individuals based on their fitness values. The value of Xp'=Xp-Xr depend on the type of termination used by genetic algorithm.

GA-based CE replacement algorithm

1. **Start Replacement**
2. **Input** $\mathbf{H}_i^p$, $\mathbf{H}_i^c$, and $\mathbf{H}_i^m$
3. $\mathbf{H}_i^R = [\mathbf{H}_i^p, \mathbf{H}_i^c, \mathbf{H}_i^m]$
4. **For** j=1: 50.5*Xpp
5. FitVal (j) = $|\mathbf{Y}p - \mathbf{H}_{ij}^R \mathbf{X}p|^2$
6. **End For**
7. Xp'=Xp-Xr
8. **For** k=1: Xp'
9. [a, b] = **min** (FitVal)
10. $\mathbf{H}_{(i+1)k} = \mathbf{H}_{ib}^R$
11. FitVal (b) = 1000
12. **End For**
13. **Output** $\mathbf{H}_{i+1}$
14. **End Replacement**

The value of Xr determines the convergence of the algorithm. For Xr=0 all the generations have equal number of individuals and the value of Yg is fixed. But for Xr≠0 each new generation's number of individuals decreased by Xr. It is mainly used to avoid repetition of individuals and hence to reduce complexity.

5.3 MUD Algorithm

5.3.1 Introduction

After channel estimation is performed by the channel estimator, the next step is the data detection phase. The formula that relates the received data signal with the transmitted data signal is mentioned in Equation (5.19). The equation describes the transmitted signal, $\mathbf{x_d}$, is corrupted by two factors, the AWGN, $\mathbf{z}$, and the effect of inter user interference, $\mathbf{H}$.

$$\mathbf{y_d} = \mathbf{H}\mathbf{x_d} + \mathbf{z} \tag{5.19}$$

Using Equation (5.7) it is possible to expand Equation (5.19) for transmission of one symbol at a time. The modulation method of the transmitted bits $\mathbf{b_i^c}$ is 16-QAM, i.e. one symbol x_i is used to represent four bits. The user bits, $\mathbf{b_i^c}$ for i=1 … 4, are modulated and represented by x_{di}, i=1 … 4 and then transmitted through the wireless channel.

$$\begin{bmatrix} \mathbf{b_1^c} \\ \mathbf{b_2^c} \\ \mathbf{b_3^c} \\ \mathbf{b_4^c} \end{bmatrix} = \begin{bmatrix} b_{11}^c & b_{12}^c & b_{13}^c & b_{14}^c \\ b_{21}^c & b_{22}^c & b_{23}^c & b_{24}^c \\ b_{31}^c & b_{32}^c & b_{33}^c & b_{34}^c \\ b_{41}^c & b_{42}^c & b_{43}^c & b_{44}^c \end{bmatrix} \tag{5.20}$$

$$\begin{bmatrix} \mathbf{b_1^c} \\ \mathbf{b_2^c} \\ \mathbf{b_3^c} \\ \mathbf{b_4^c} \end{bmatrix} \xrightarrow{\text{Modulation}} \begin{bmatrix} x_{d1} \\ x_{d2} \\ x_{d3} \\ x_{d4} \end{bmatrix} \tag{5.21}$$

$$\begin{bmatrix} y_{d1} \\ y_{d2} \end{bmatrix} = \begin{bmatrix} h_{11} & h_{12} & h_{13} & h_{14} \\ h_{21} & h_{22} & h_{23} & h_{24} \end{bmatrix} \begin{bmatrix} x_{d1} \\ x_{d2} \\ x_{d3} \\ x_{d4} \end{bmatrix} + \begin{bmatrix} z_1 \\ z_2 \end{bmatrix} \tag{5.22}$$

The MUD is used to estimate the transmitted signals by reversing the effect of the transmission channel using the output of CE and by reducing the effect of noise at the transmission. The following sections describe the general operations performed in GA-based MUD.

5.3.2 GA-based MUD

The main steps used by GA-based MUD are initialization, selection, crossover, mutation and finally replacement operations which are performed to reduce the sample space and select the best fit individual. The order of the operators is the same as that of the GA-based CE algorithm and the only difference is that GA-based MUD uses binary representation in the algorithm. The main parameters used by the algorithm are:

- Nx - Number of individuals in a generation,
- Ny - Total number of generations,
- Nr - Replacement convergence size, and
- Nt – Number of tournament groups.

The pseudocode that illustrates the main steps of GA-based MUD is given below and each of the operators in the algorithm will be elaborated in the following topics.

GA-based MUD algorithm

1. **Start GAMUD**
2. **Initialize** $\mathbf{B}_1$
3. **For** i=1: Ny
4. **Select** Ns individuals
5. **Crossover** selected individuals
6. **Mutation** of the children
7. **Replacement** of weak parents
8. **End For**
9. **Output** $\widehat{\mathbf{B}}$
10. **End GAMUD**

5.3.2.1 Initialization

The representation of the individual chromosome **B** is based on bits with M=4 rows, each represent the potential user, and modulation order=4 columns, because the system uses 16-QAM, i.e. there are 16 modulating symbols and 4 bits per symbol. There are 16 bits in **B**, each bit represents one gene in the individual. Representation of GA-based MUD individual is given in Equation (5.23).

$$\mathbf{B} = \begin{bmatrix} b_{11} & b_{12} & b_{13} & b_{14} \\ b_{21} & b_{22} & b_{23} & b_{24} \\ b_{31} & b_{32} & b_{33} & b_{34} \\ b_{41} & b_{42} & b_{43} & b_{44} \end{bmatrix} \tag{5.23}$$

The first generation of the algorithm is constructed from initialization, based on random initialization of bit streams. There are Nx individuals in the first generation, which determines the accuracy of the estimated data and the convergence time.

The result of initialization operation is feed to the selection stage. There are $2^{(M*ModOrd)} = 2^{16} = 65{,}536$ combinations or number of individuals in the sample space. Some of the values used in the algorithm are Nx = 32,768, 16,384, 8,192 … 256 or $2^{(M*ModOrd-j)}$ randomly initialized individuals for j=1, 2 … 8. The set of individuals after the initialization stage is given in Equation (5.24).

$$\mathbf{B}_0 = [\mathbf{B}_{01}, \mathbf{B}_{02} \ldots \mathbf{B}_{0Nx}] \tag{5.24}$$

5.3.2.2 Selection

The inputs to selection stage are individuals from initialization or replacement operations. The selection method used in GA-based MUD is tournament selection and there are Nt tournament groups which divides based on their order.

Using rank selection Ns/Nt best elements are selected at each group of Nx/Nt individuals and results in Ns elements transferred for the next step. The pseudocode that describes tournament selection operation is given below.

GA-based MUD selection algorithm

1. **Start Selection**

2. **Input** $\mathbf{B}_i$, $\mathbf{H}$, and $\mathbf{y}_d$

3. **For** j=1: Nx

4. Modulate $\mathbf{B}_{ij}$ to $\mathbf{x}_j$

5. FV (j) = $|\mathbf{y}_d - \mathbf{H}\mathbf{x}_j|^2$

6. **End For**

7. **Initialize** Nt and Ns

8. **For** k=1: Nt

9. **For** l=1: Ns/Nt

10. [a, b] = **min** (FV ((k-1)*Nx/Nt+1: k*Nx/Nt))

11. $\mathbf{B}^{\mathbf{s}}_{\mathbf{i}((\mathbf{k}-\mathbf{1})*\frac{\mathbf{Ns}}{\mathbf{Nt}}+\mathbf{l})} = \mathbf{B}_{\mathrm{i}((\mathrm{k}-1)*\frac{\mathrm{Nx}}{\mathrm{Nt}}+\mathrm{b})}$

12. FV ((k-1)*Nx/Nt + b) = 1000

13. **End For**

14. **End For**

15. **Output** $\mathbf{B}_i^s$

16. **End Selection**

The result of selection operation is $\mathbf{B}^s$, a set of selected individuals from each tournament group. All the individuals in the set $\mathbf{B}^s$ will be given in Equation (5.25).

$$\mathbf{B}_i^s = [\mathbf{B}_{i1}^s, \mathbf{B}_{i2}^s \ldots \mathbf{B}_{iNs}^s] \quad (5.25)$$

5.3.2.3 Crossover

One point crossover is used as a binary crossover technique where the selected individuals in the population combine their genes to form the newly born children. Let

the two parents are $\mathbf{B_1}$ and $\mathbf{B_2}$ are selected randomly from the set of selected individuals and represented with their genes as given on Equation (5.26). Crossover point is selected randomly to identify the crossing border. Crossover of individuals $\mathbf{B_1}$ and $\mathbf{B_2}$ with crossover point 2 gives two children, $\mathbf{B}_1^c$ and $\mathbf{B}_2^c$ as given in Equation (5.27).

$$\mathbf{B_1} = \begin{bmatrix} b_{11} & b_{12} & b_{13} & b_{14} \\ b_{21} & b_{22} & b_{23} & b_{24} \\ b_{31} & b_{32} & b_{33} & b_{34} \\ b_{41} & b_{42} & b_{43} & b_{44} \end{bmatrix} \quad \text{and} \quad \mathbf{B_2} = \begin{bmatrix} b'_{11} & b'_{12} & b'_{13} & b'_{14} \\ b'_{21} & b'_{22} & b'_{23} & b'_{24} \\ b'_{31} & b'_{32} & b'_{33} & b'_{34} \\ b'_{41} & b'_{42} & b'_{43} & b'_{44} \end{bmatrix} \tag{5.26}$$

$$\mathbf{B}_1^c = \begin{bmatrix} b_{11} & b_{12} & b'_{13} & b'_{14} \\ b_{21} & b_{22} & b'_{23} & b'_{24} \\ b_{31} & b_{32} & b'_{33} & b'_{34} \\ b_{41} & b_{42} & b'_{43} & b'_{44} \end{bmatrix} \quad \text{and} \quad \mathbf{B}_2^c = \begin{bmatrix} b'_{11} & b'_{12} & b_{13} & b_{14} \\ b'_{21} & b'_{22} & b_{23} & b_{24} \\ b'_{31} & b'_{32} & b_{33} & b_{34} \\ b'_{41} & b'_{42} & b_{43} & b_{44} \end{bmatrix} \tag{5.27}$$

The main steps performed in crossover operation are given below.

GA-based MUD crossover algorithm

1. **Start Crossover**
2. **For** j=1: Ns/2
3. **Select** $\mathbf{B}_{ij}^s$ and $\mathbf{B}_{i(\frac{Ns}{2}+j)}^s$ from $\mathbf{B}_i^s$
4. **Choose** crossover point x_p
5. $\mathbf{B}_{ij}^c(:, 1: x_p) = \mathbf{B}_{ij}^s(: , 1: x_p)$
6. $\mathbf{B}_{i(\frac{Ns}{2}+j)}^c(:, 1: x_p) = \mathbf{B}_{i(\frac{Ns}{2}+j)}^s(: , 1: x_p)$
7. $\mathbf{B}_{ij}^c(:, x_p+1:\text{ModOrd}) = \mathbf{B}_{i(\frac{Ns}{2}+j)}^s(: , x_p+1:\text{ModOrd})$
8. $\mathbf{B}_{i(\frac{Ns}{2}+j)}^c(:, x_p+1:\text{ModOrd}) = \mathbf{B}_{ij}^s(: , x_p+1:\text{ModOrd})$
9. **End For**
10. **End Crossover**

The result of crossover operation is a set of children with the same number as the result of the selection stage Ns=Nc. The set is given in Equation (5.28).

$$\mathbf{B}_i^c = [\mathbf{B}_{i1}^c, \mathbf{B}_{i2}^c \ \ldots \ \mathbf{B}_{iNc}^c] \tag{5.28}$$

5.3.2.4 Mutation

Mutation operation is performed based on random selection of one bit and change the bit to the reverse value. Let the j^{th} child is $\mathbf{B}_{ij}^{c}$ for j=1, 2 … Nc one of the gene of the child is selected and its value is changed to form the new child.

GA-based MUD mutation operation

1. **Start Mutation**
2. **For** j=1: Nc
3. **Select** the j^{th} child $\mathbf{B}_{ij}^{c}$
4. **Select** one of the gene b randomly
5. **If** b==0
6. b'=1
7. **Else**
8. b'=0
9. **End If**
10. b_{ij}^{m} =b'
11. **End For**
12. **End Mutation**

Mutation operation generates Nm individuals as given in Equation (5.29).

$$\mathbf{B}_{i}^{m} = [\mathbf{B}_{i1}^{m}, \mathbf{B}_{i2}^{m} \ \dots \ \mathbf{B}_{iNm}^{m}] \tag{5.29}$$

5.3.2.5 Replacement

The replacement operation is performed based on the rank selection. Collect the individuals in the selected parent population, children from crossover operation and mutation operation as given in Equation (5.30). The total number of individuals to be analyzed is Nxt=Ns+Nc+Nm=3*Ns because Ns=Nc=Nm.

$$\mathbf{B}_{i}^{T} = [\mathbf{B}_{i}^{s}, \mathbf{B}_{i}^{c}, \mathbf{B}_{i}^{m}] = [\mathbf{B}_{i1}^{s}, \mathbf{B}_{i2}^{s} \dots \mathbf{B}_{iNs}^{s}, \mathbf{B}_{i1}^{c}, \mathbf{B}_{i2}^{c} \ \dots \ \mathbf{B}_{iNc}^{c}, \mathbf{B}_{i1}^{m}, \mathbf{B}_{i2}^{m} \ \dots \ \mathbf{B}_{iNm}^{m}] \tag{5.30}$$

The best Nx'=Nx*Nr individuals are selected based on their fitness values. The main steps performed in the replacement operation are given below.

GA-based MUD replacement algorithm

1. **Start Replacement**
2. $\mathbf{B}_i^T = [\mathbf{B}_i^s, \mathbf{B}_i^c, \mathbf{B}_i^m]$
3. **For** j=1:3*Ns
4. Modulate $\mathbf{B}_{ij}^T$ **to** $\mathbf{x}_j$
5. FV (j) = $|\mathbf{y}_d - \mathbf{H}\mathbf{x}_j|^2$
6. **End For**
7. k=1; Nx'=Nx*Nr;
8. **While** (k<=Nx')
9. [a, b] = **min** (FV);
10. Fvx (k) = a;
11. **If** (k==1)
12. $\mathbf{B}_{i1}^r = \mathbf{B}_{ib}^T$;
13. **Else**
14. **If** (Fvx (k) == Fvx (k-1))
15. FV (b) = 1000;
16. **Continue**;
17. **Else**
18. $\mathbf{B}_{ik}^r = \mathbf{B}_{ib}^T$;
19. **End If**
20. **End If**
21. k = k+1;
22. **End While**
23. **Output** $\mathbf{B}_i^r$
24. **End Replacement**

GA-based MUD replacement algorithm has a special future used to remove reputations of individuals with the same fitness values. The output of the replacement operation is represented in Equation (5.31).

$$\mathbf{B}_{i+1} = \mathbf{B}_i^r = [\mathbf{B}_{i1}^r, \mathbf{B}_{i2}^r \ldots \mathbf{B}_{iNx'}^r] \quad (5.31)$$

5.4 General Algorithm

The uplink system algorithm design is based on the overall operations performed in the uplink communication system given on Figure 5.1. The algorithm includes user data generation, channel encoding, modulation, and transmission phases at the transmitter and GA-based JCEMUD, channel decoding and performance analysis at the receiver. The overall uplink system algorithm in pseudocode is given below.

Uplink system algorithm

1. **Start GA-JCEMUD**
2. **For** iSNR=0:3:30
3. **For** iRept=1:NumRep
4. **Generate** $\mathbf{B}_T$
5. **Bc**=**encode**($\mathbf{B}_T$)
6. **X**m=**modulate**(**B**c)
7. **For** i=1: nSymbols/nFrames
8. $\mathbf{Y}_p$ = **HX**p + **Z**(iSNR)
9. $\widehat{\mathbf{H}}$ = **GACE**($\mathbf{Y}_p$, **X**p, Yg, Xp, Xr)
10. **For** j=1: nFrames
11. $\mathbf{y}_d$ = **HX**m(:, (i-1)*nFrames+j) + **z**(iSNR)
12. $\widehat{\mathbf{B}}$ = **GAMUD**($\mathbf{y}_d$, $\widehat{\mathbf{H}}$, Ny, Nx, Nr)
13. $\widehat{\mathbf{B}}$**c**(:, ((i-1)*4*nFrames+(j-1)*4+1:(i-1)*4*nFrames+j*4))= $\widehat{\mathbf{B}}$
14. **End For**
15. **End For**
16. $\widehat{\mathbf{B}}_T$ = **decode**($\widehat{\mathbf{B}}$**c**)
17. BitErr = BitErr + **biterr**($\mathbf{B}_T$, $\widehat{\mathbf{B}}_T$)
18. **END For**
19. BER(iSNR)=BitErr/(NumRep*nSymbols*16)
20. **End For**
21. **End GA-JCEMUD**

CHAPTER 6

SIMULATION RESULTS

6.1 Evaluation Metrics

The evaluation of different CE and MUD methods is performed based on their performance and complexity. Performance is measured based on bit error rate or mean square error values at different signal-to-noise ratio points.

SNR is a measure used in communication engineering that compares the level of a desired signal to the level of background noise. It is defined as the ratio of signal power P_s to the noise power P_n, often expressed in decibels.

$$SNR = 10\log\frac{P_s}{P_n} = P_s\,(dB) - P_n\,(dB) \tag{6.1}$$

BER indicates the total number of error bits per total number of transmitted bits of all transmitter antennas. Unless specified BER in this thesis indicates *information BER*, i.e. the number of decoded bits that remain incorrect after the error correction, divided by the total number of decoded bits.

MSE is the second moment of the error and thus incorporates both the variance of the estimator and its bias. For CE algorithms MSE can be represented in Equation (6.2) and for MUD methods MSE is calculated from Equation (6.3).

$$MSE_{CE} = \frac{1}{N}\sum_{i=1}^{N} |\mathbf{H} - \widehat{\mathbf{H}}|^2 \tag{6.2}$$

$$MSE_{MUD} = \frac{1}{N}\sum_{i=1}^{N} |\mathbf{x} - \hat{\mathbf{x}}|^2 \tag{6.3}$$

Evaluation of an algorithm is also done by factors which include rate of convergence and computational complexity. Rate of convergence is defined as the number of iterations required for the algorithm, in response to stationary inputs, to converge close enough to the optimum solution. Computational complexity is the number of computations required to make one complete estimation of the algorithm [3].

6.2 Performance Measurement

Performance of each CE and MUD methods are analyzed based on their BER-SNR and MSE-SNR curves. First it is necessary to compare different CE and MUD methods independently and then the comparison will be performed by combining CE and MUD methods together.

6.2.1 Channel estimation

For GA-based CE algorithm given in Section 5.2 proper Yg, Xp, Xrt and Xr values should be chosen in initialization, selection and replacement operations. These values determine the accuracy and complexity of the algorithm. Xp + 50.5XrtXp individuals are analyzed at each iteration and number of individuals decreased by Xr per iteration. Total number of individuals analyzed for each GA-based CE stage is given in Equation (6.4).

X_{Tot} = (Xp + 50.5XrtXp) + ((Xp-Xr) + 50.5Xrt*(Xp-Xr)) + … + ((Xp-(Yg-1)*Xr) + 50.5Xrt*(Xp-(Yg-1)*Xr))

= Xp*(1 + 50.5Xrt) + (Xp-Xr)*(1 + 50.5Xrt) + … + (Xp-(Yg-1)*Xr)*(1 + 50.5Xrt)

= (1 + 50.5Xrt)*(Xp + (Xp-Xr) + … + (Xp-(Yg-1)*Xr)

= (1 + 50.5Xrt)*(YgXp – (Xr + 2Xr + … + (Yg-1)*Xr)

= (1 + 50.5Xrt)*(YgXp - $\sum_{ig=1}^{Yg-1} ig * Xr$)

$$X_{Tot} = (1 + 50.5Xrt)*(YgXp - \sum_{ig=1}^{Yg-1} ig * Xr) \quad (6.4)$$

For Xr=0 total number of individuals analyzed will be given in Equation (6.5).

$$X_{Tot} = (1 + 50.5Xrt)*(YgXp) \quad (6.5)$$

From Equation (6.4) total number of individuals analyzed, X_{Tot}, is determined by the values of Xp, Yg, Xrt, and Xr at each operations. But there are no predefined rules to select the values of the parameters. Therefore, it is necessary to plot cost value curves for each variables and select the value that optimize accuracy with acceptable computational complexity.

To determine the value of Yg that gives minimum fitness value with tolerable complexity, it is necessary to know the relation between Yg and fitness value. The plot of fitness value - Yg curve for Xp=1000, Xrt=0.2, Xn=20, Xr=0; and SNR=0, 10, and 30 dB is given in Figure 17 below. Total number of individuals per estimation is X_{Tot} = (1 + 50.5*0.2)*(1000Yg) = 11,100Yg.

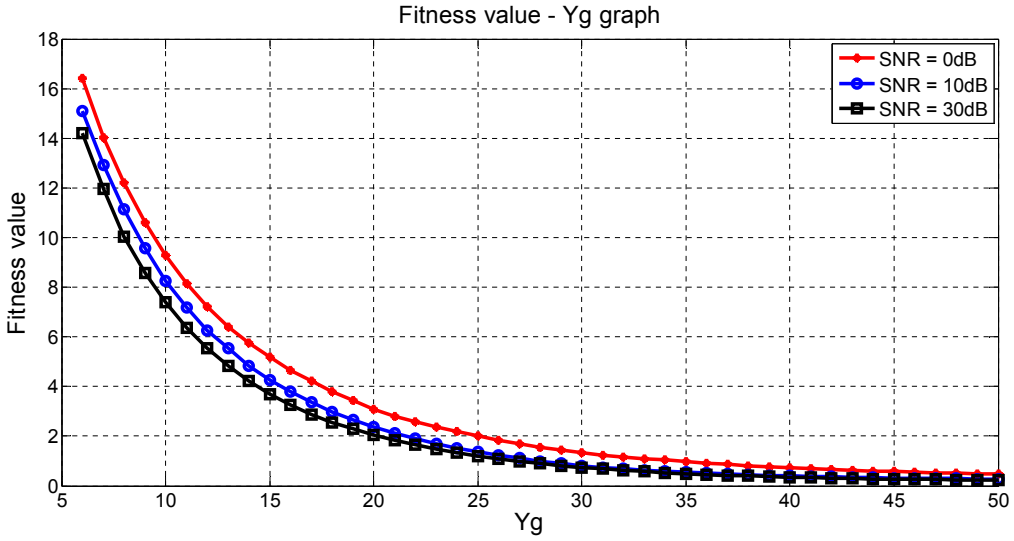

Figure 17: Fitness value - Yg curves for Xp=1000.

Fitness values at different Yg and SNR points are listed in Table 9.

Yg	Fitness value at 0dB	Fitness value at 10dB	Fitness value at 30dB
6	16.3965	15.0889	14.2291
10	9.2825	8.2387	7.5772
20	3.0966	2.3641	2.0811
30	1.3385	0.8158	0.7039
40	0.7313	0.3983	0.3229
50	0.4757	0.2726	0.1974

Table 9: Fitness values at different Yg and SNR points.

From Figure 17 the rate of change of fitness values decreases as Yg increases. For Yg=10, 20, 30, 40, 45, and 50 values, average slope values of the curves are 1.1863, 0.2808, 0.0846, 0.0268, 0.0163, and 0.0055 respectively.

Plot of fitness value - Xp curve for Yg=30, Xrt=0.2, Xr=0; and SNR=0 and 30 dB is given in Figure 18. From Equation (6.5) total number of individuals processed is X_{Tot} = (1+50.5*0.2)*(30Xp) = 333Xp.

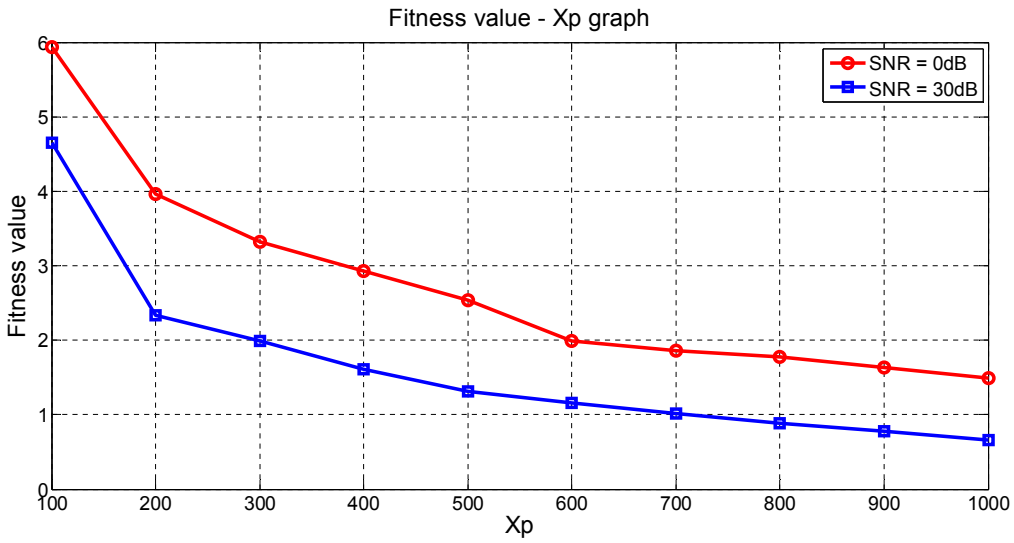

Figure 18: Fitness value - Xp curves for Yg=30.

Table below shows fitness values at different SNR and Xp values.

Xp	X_{Tot}	Fitness value at 0dB	Fitness value at 30dB
200	66,600	3.9608	2.3282
400	133,200	2.9266	1.5005
600	199,800	1.9843	1.1249
800	266,400	1.7746	0.9003
1000	333,000	1.4887	0.8529

Table 10: Fitness values at different Xp and SNR points.

Figure 18 shows that fitness value decreases as Xp value increases and slope of fitness value curve decreases as the value of Xp increases. Rate of change of fitness values between 100-200, 200-600, and 600-1000 are 0.0213, 0.0039, and 0.00096 respectively. This indicates that as number of individuals increase above 600 change in fitness value decreases and complexity increases. To decrease the complexity of GA-based CE it is necessary to improve the previous algorithm by making Xr≠0.

To select the best Xr value the plot of fitness value - Xr gives good observation. For fixed Xp and Xr≠0, Yg varies based on Xr, i.e. for Yg iterations in GA-based CE algorithm Xp – XrYg > 0 and this gives Yg < Xp/Xr. This implies that Yg = (Xp/Xr) - 1. Figure 19 gives the relation between fitness value and Xr at Xp=800 and Xrt=0.2. For Xr=0 Yg=50 and for Xr≠0 Yg = (Xp/Xr) – 1. Total number of generations including the initial generation is Y_{Tot} = Yg+1 = Xp/Xr.

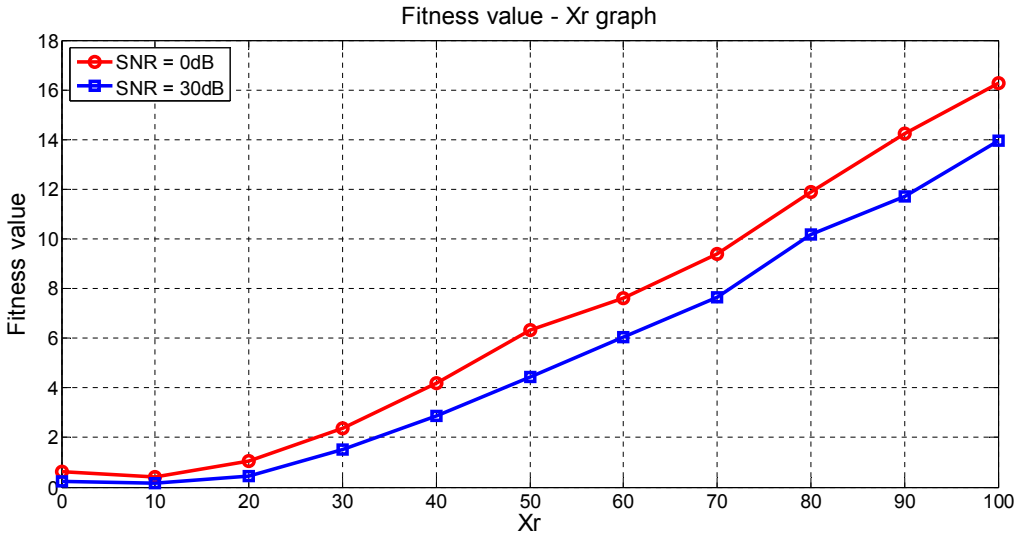

Figure 19: Fitness value - Xr graph for Xp=800.

From Figure 19 the following fitness values are selected for different Xr values.

Xr	Y_{Tot}	X_{Tot}	Fitness value at 0dB	Fitness value at 30dB
0	51	444,000	0.6400	0.2358
20	40	181,818	1.0354	0.4559
40	20	92,796	4.1884	2.8749
60	14	63,492	7.6202	6.0401
80	10	47,952	11.8862	10.1792
100	8	38,850	16.2542	13.9654

Table 11: MSE and total population used for each Xr values

Therefore, as the value of Xr increases total number of generations Yg decreases and the slope of fitness value increases and as a result the accuracy of the algorithm decreases. To observe the variation of fitness value for different Xp values, the graph below gives fitness value - Xp relation for fixed value of Xr=20 and Y_{Tot}=Xp/Xr.

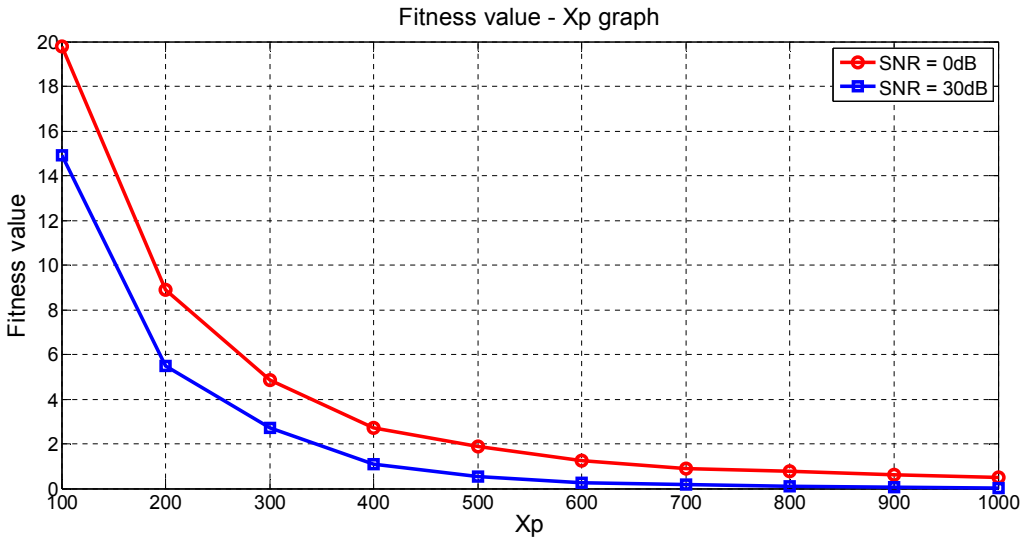

Figure 20: Cost-Xp graph for Xr=20

The following fitness values are selected from Figure 20.

Xp	X_{Tot}	Fitness value at 0dB	Fitness value at 30dB
200	11,988	8.8998	5.4931
400	46,398	2.7005	1.0742
600	103,008	1.2345	0.2745
800	181,818	0.7566	0.0912
1000	282,828	0.4993	0.0323

Table 12: Variation of fitness value with Xp and SNR for Xr≠0

From Figure 20 and Table 12 for **Xp=800** initial population use of **Xr=20** decreases the complexity of the algorithm by reducing the whole population analyzed from **444,000** to **181,818**. Total number of individuals used is reduced by **262,182** individuals with total generation of $\mathbf{Y_{Tot}=40}$. Generally use of **Xp=800** with **Xr=20** and $\mathbf{Y_{Tot}=40}$ gives relatively good result with better performance and small complexity.

GA-based CE method is compared with LS and MMSE channel estimation methods using ML data detection. GA-based CE is simulated based on the following values: **Xp=800**, **Xr=20**, $\mathbf{Y_{Tot}=40}$, **Xrt=0.2** and **Xn=20**. BER-SNR graph given below shows the performance of GA, LS, and MMSE channel estimation methods without channel coding.

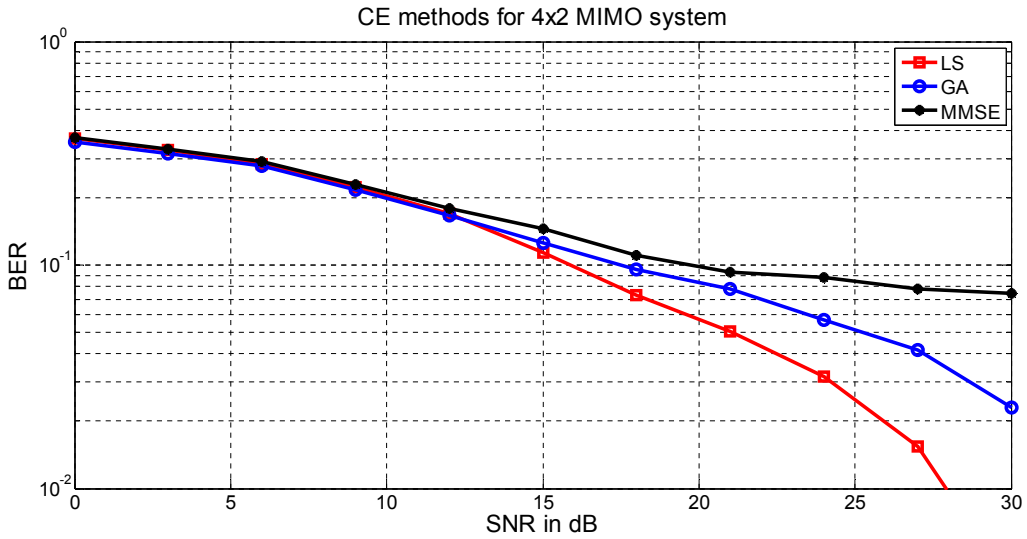

Figure 21: BER-SNR graph for LS, GA, and MMSE CE methods.

Some of BER values are given on Table 13.

SNR in dB	BER value of LS	BER value of GA	BER value of MMSE
6	0.2836	0.2785	0.2913
9	0.2233	0.2164	0.2287
12	0.1700	0.1669	0.1794
15	0.1135	0.1252	0.1448
18	0.0734	0.0952	0.1102

Table 13: BER values at specific SNR points.

From **0-12**dB GA-based CE method is superior to other channel estimation methods. The slope of BER curve decreases as SNR increases due to inter-user interference. LS channel estimation method is implemented by using orthogonal decomposition methods like QR-decomposition or singular value decomposition methods. Generally using the LS CE method is slower than GA-based CE method but LS CE method is more numerically stable.

Using Equation (6.2) MSE of LS and GA-based CE methods is computed to further analyze the performance between 0 and 30dB SNR points. MSE-SNR curves for LS and GA-based CE methods are given on Figure 22 below.

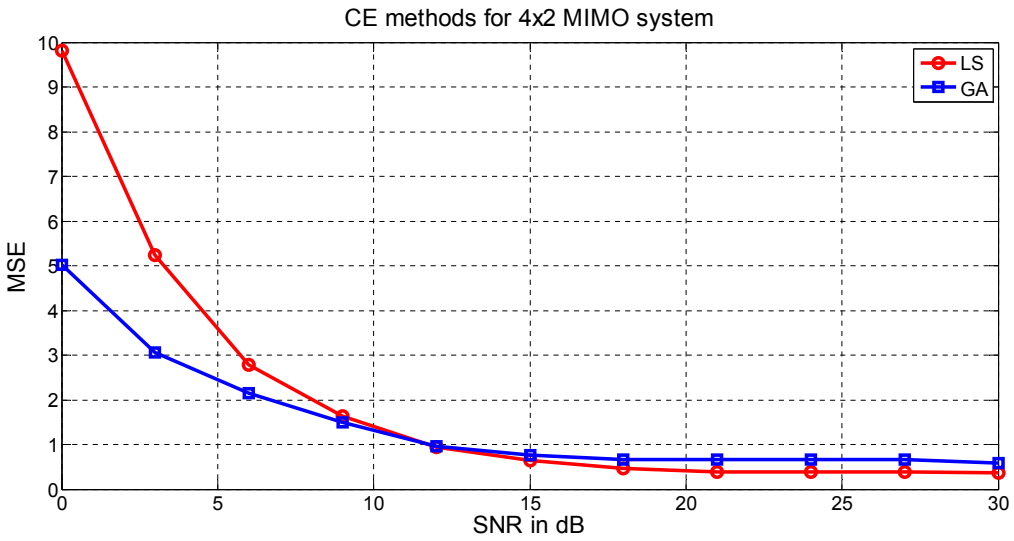

Figure 22: MSE-SNR graph for GA and LS CE methods.

MSE values at different SNR points are given on Table 6.4.

SNR in dB	MSE value of LS	MSE value of GA	ΔMSE
0	9.2712	4.8585	4.4127
6	2.8710	2.3316	0.5394
12	0.9548	0.9294	0.0254
18	0.6290	0.6771	-0.0481
24	0.4035	0.6010	-0.1977
30	0.3725	0.5812	-0.2087

Table 14: MSE values for LS, GA, and MMSE CE methods

From the results given on Figure 22 the following observations are made. Between 0-12dB MSE performance of GA is superior with average MSE value of 1.54 and above 12dB LS has better performance with average of 0.22. Therefore, GA-based CE has better performance for low SNR communication and score good performance at normal communication systems.

6.2.2 GA-based MUD

Performance of MUD methods given in Chapter 3 and GA-based MUD method in Section 5.3 is analyzed based on their BER and MSE values at a range of SNR points. MSE value of all individuals in the sample space is plotted on Figure 23 using Equation (6.3). MSE value of individuals varies between **0** and **208**.

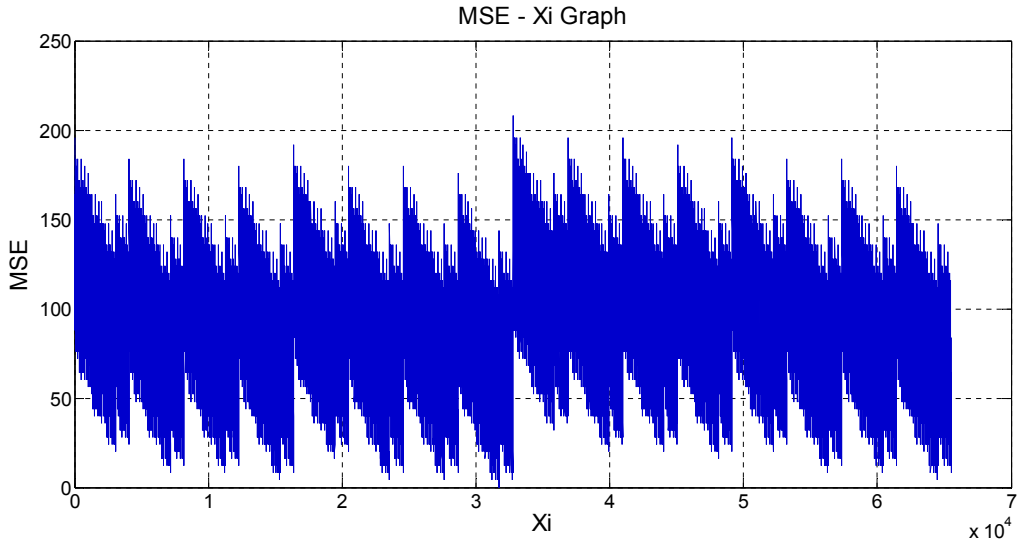

Figure 23: MSE-Xi graph.

Based on GA-based MUD algorithm given in Section 5.3.2 total number of individuals analyzed per each data estimation stage, N_{Tot}, is given on Equation (6.6).

$$N_{Tot} = (Nx+3Ns) + (Nx*Nr+3Ns*Nr) + (Nx*Nr^2+3Nx*Nr^2) + \dots + (Nx*Nr^{Ny-1}+3Nx*Nr^{Ny-1})$$

$$= (Nx+3Ns)*(1 + Nr + Nr^2 + \dots + Nr^{Ny-1})$$

$$= (Nx+3Ns)\sum_{iy=0}^{Ny-1} Nr^{iy}$$

$$N_{Tot} = (Nx+3Ns)\sum_{iy=0}^{Ny-1} Nr^{iy} \quad (6.6)$$

Total number of individuals, N_{Tot}, and as a result complexity and accuracy of GA-based MUD depends on Nx, Ns, Ny, and Nr values in the algorithm. To select best values of these parameters it is necessary to plot their fitness curves using Equation (6.7).

$$\text{Fitness value} = |\mathbf{Y_d} - \mathbf{H}*\mathbf{X_{est}}|^2 \quad (6.7)$$

For Ny=2, Nr=0.1, Ns=0.1Nx, and Nt=0.05Nx values total number of individuals analyzed is N_{Tot}=Nx*(1+0.3)*(1+0.1) = Nx*1.3*1.1=1.43Nx. The graph that shows the relation between fitness value and Nx is given in Figure 24.

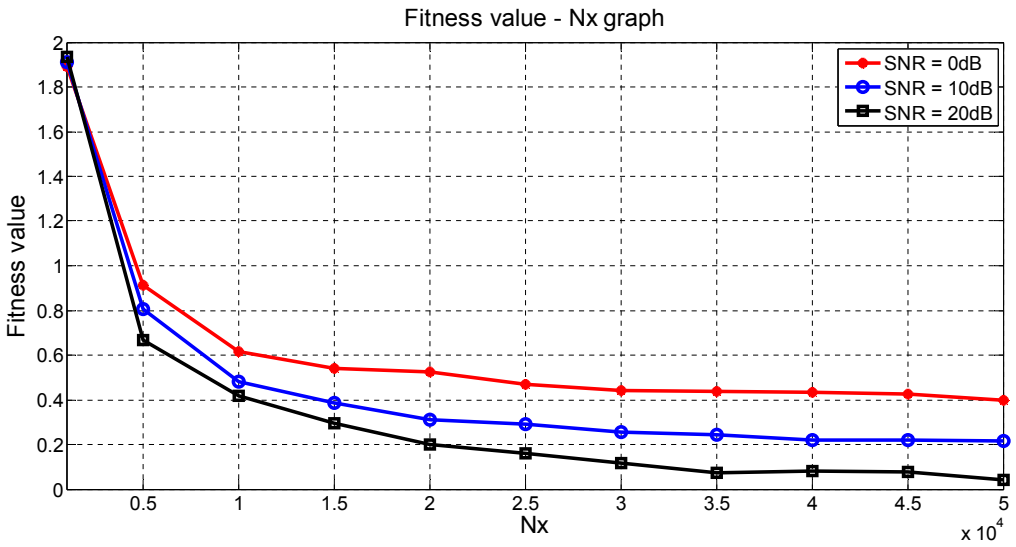

Figure 24: Fitness value-Nx graph for Ny=2.

Table 15 gives total number of individuals analyzed and fitness values for different Nx values and at different SNR points.

Nx	N_{Tot}=1.43Nx	Fitness value at 0dB	Fitness value at 10dB	Fitness value at 20dB
1,000	1430	1.8894	1.9196	1.9337
10,000	14,300	0.6174	0.4817	0.4191
20,000	28,600	0.5254	0.3095	0.1992
30,000	42,900	0.4409	0.2542	0.1181
40,000	57,200	0.4331	0.2203	0.0793
50,000	71,500	0.3999	0.2170	0.0425

Table 15: Fitness values at specific Nx points.

From Figure 24 average slope of curves between 1000-10000, 10000-30000, and 30000-50000 Nx values are 0.16, 0.012, and 0.0026 per 1000 individuals respectively. These results show that above Nx=30000 rate of change of error power is approximately zero and **Nx=30000** gives acceptable fitness value with smaller complexity.

For Nx=10000, Ns=0.4Nx, and Nr=0.6 N_{Tot} = (Nx+3Ns)* $\sum_{iy=0}^{Ny-1} Nr^{iy}$ = 2.2Nx*$\sum_{iy=0}^{Ny-1} 0.6^{iy}$ = 22000$\sum_{iy=0}^{Ny-1} 0.6^{iy}$. The graph that shows the relation between fitness value and SNR for Ny = 0, 1, and 2 is given in Figure 25 below.

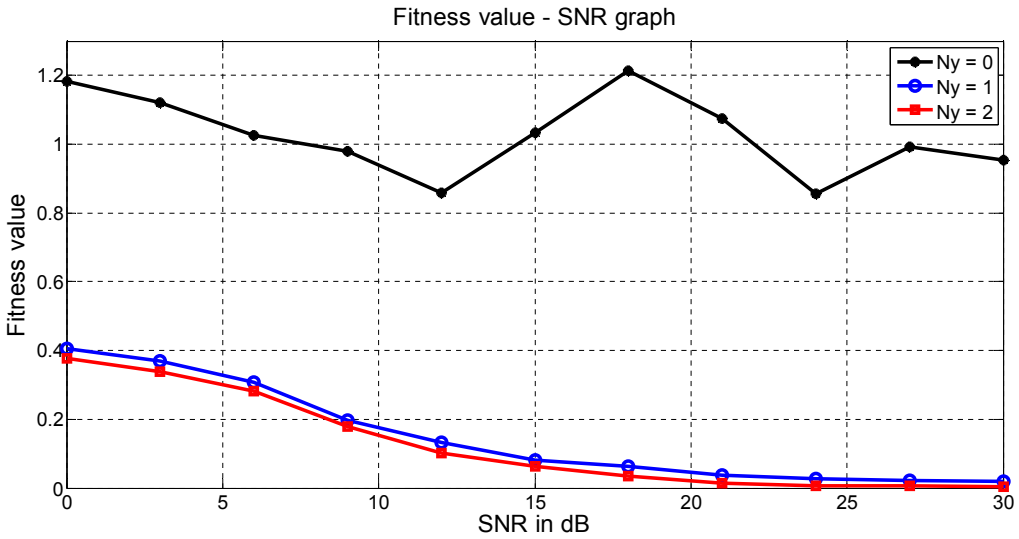

Figure 25: Fitness value-SNR curves for Ny = 0, 1, and 2.

Some of fitness values for different number of generations and SNR values are given in Table 16.

Ny	N_{Tot}	Fitness value at 0dB	Fitness value at 15dB	Fitness value at 30dB
0	10,000	1.1830	1.0337	0.9527
1	22,000	0.4057	0.0817	0.0185
2	35,200	0.3780	0.0618	0.0027

Table 16: Fitness values at specific SNR points.

For Ny=0, the initial population of the algorithm, average minimum fitness value of all SNR points is **1.0264** and it does not depend on SNR value. Average change of fitness values from initial population to first generation and from first generation to second generation are **0.8753** and **0.0232** respectively. This result shows that the algorithm gives almost similar result for Ny>=2. Therefore, selecting **Ny=2** gives acceptable accuracy with minimum complexity.

By using the best values determined in the previous simulations it is possible to plot BER-SNR and MSE-SNR curves of different CE methods by assuming perfect CSI at the receiver. GA-based MUD is simulated using Nx=30,000, Ny=2, Ns=0.1Nx, and Nr=0.1 with total population N_{Tot} = Nx*(1+0.3)*(1+0.1) = Nx*1.3*1.1 = 1.43Nx=42,900. Figure 26 compares GA, ZF, MMSE, and ML MUD methods for M=4 and N=2.

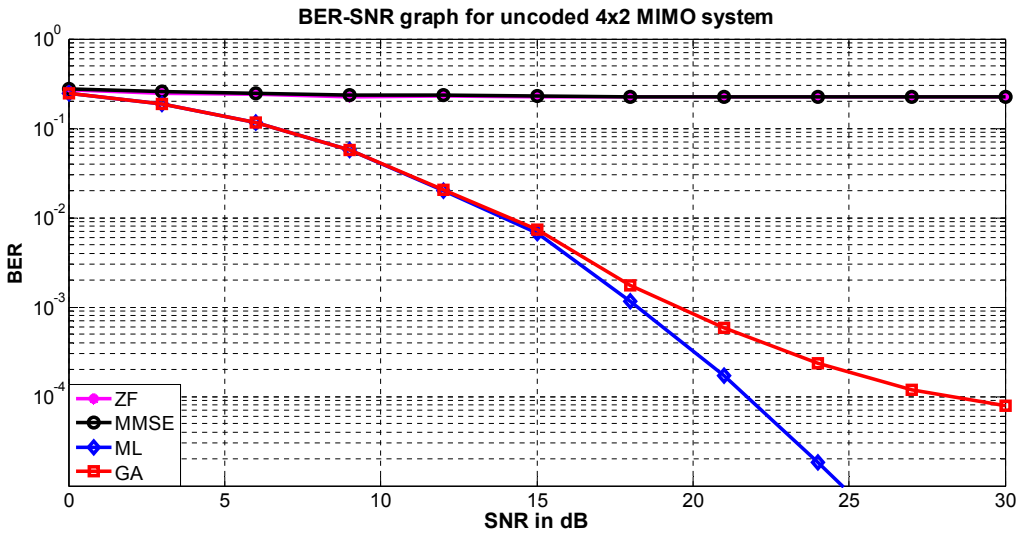

Figure 26: BER-SNR curves of MUD methods with full CSI.

Some of BER values at specific SNR points are listed in Table 17.

SNR in dB	BER value of ML	BER value of GA	BER value of MMSE	BER value of ZF
9	0.05736	0.05773	0.23556	0.22693
12	0.01998	0.02043	0.23270	0.22959
15	0.00670	0.00742	0.22864	0.22639
18	0.00115	0.00176	0.22664	0.22617
21	0.00017	0.00058	0.22696	0.22615

Table 17: BER values for MUD methods with full CSI.

From performance comparison given in Figure 26, ZF and MMSE MUD methods can't used for overloaded receiver due to their low BER performance at all SNR values. From **0-15dB** GA-based MUD gives the same performance as ML method but as SNR increases above 15dB performance of GA-based MUD method is lower than ML.

Plot of MSE-SNR graph for MUD methods is given in Figure 27 below. MSE value of MUD methods is calculated using Equation (6.3).

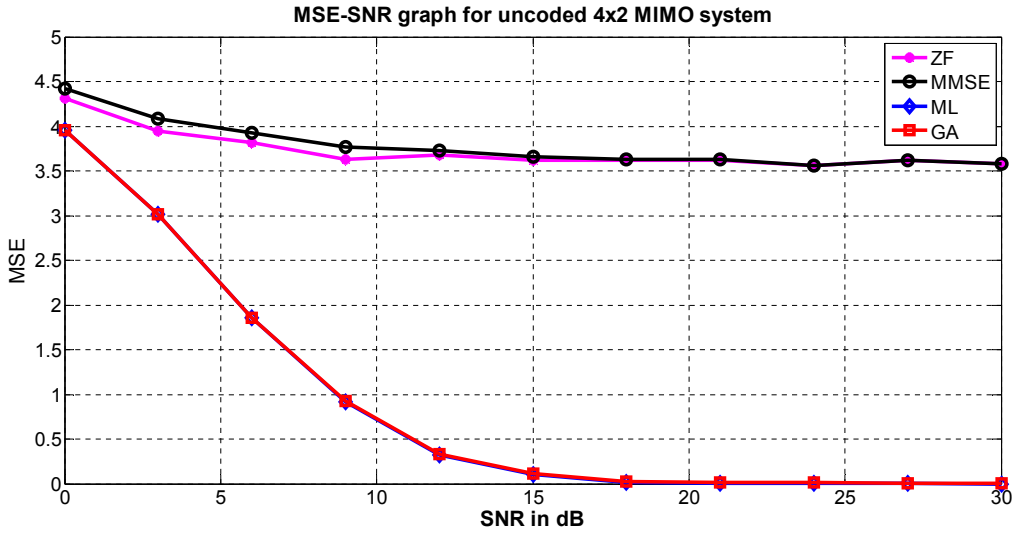

Figure 27: MSE-SNR curves for MUD methods.

MSE values of different MUD methods are given in Table 18.

SNR in dB	MSE value of ML	MSE value of GA	MSE value of MMSE	MSE value of ZF
3	3.0127	3.0172	4.0817	3.9452
9	0.9177	0.9237	3.7690	3.6310
15	0.1072	0.1187	3.6582	3.6225
21	0.0027	0.0147	3.6315	3.6185
27	0.0007	0.0094	3.6192	3.6212

Table 18: MSE values of MUD methods.

For GA-based MUD method, rate of change of MSE values per dB are **0.2557** and **0.0074** for **0-15dB** and **15-30dB** range respectively. Therefore, rate of change of BER values in log scale increase from 0dB-15dB and decrease above 15dB due to increase in SNR values increase the *interuser interference* between users.

6.2.3 GA-based JCEDD

Using GA-based CE algorithm in Section 5.2 and GA-based MUD in Section 5.3 it is possible to consruct the overall joint channel estimator and multi-user detector receiver device. The values of the parameters are the valus obtained in Sections 6.2.2 and 6.2.3

given above and are listed in Table 19. JCEDD simulation is performed based on the algorithm given in Section 5.4.

Parameter	Symbol	Value
SNR values the receiver operates with	SNR	0:3:30
Modulation type	QAM	16-QAM
Channel encoder	LDPC	R=1/4
Total number of symbols transmitted per SNR	TotSym	48,000
Number of pilot symbols per block and per transmitter	nPilots	4
Number of data symbols per block	nDataSym	40
Percentage of pilot overhead	%Pil	9.09%
Number of initial population in GA-based CE	Xp	800
Number of generations in GA-based CE	Yg	40
Number of initial population in GA-based MUD	Nx	30,000
Number of generations in GA-based MUD	Ny	2

Table 19: Parameter values for GA-based JCEDD algorithm.

Using the above parameter values and the algorithm from Section 5.4 the final result of GA-based JCEDD is given in Figure 28 below. Performance of GA-based JCEDD method is compared with LS-ML and GA-ML methods based on BER-SNR graphs.

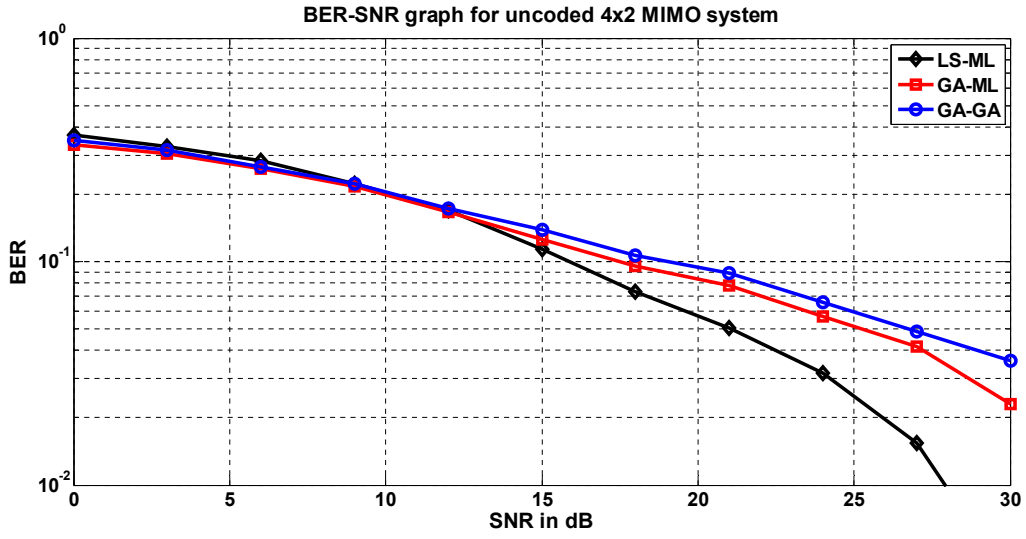

Figure 28: BER-SNR graph for JCEDD methods without coding.

BER-SNR performance of JCEDD methods with LDPC encoder is given in Figure 29. From Figure 29 and Table 20 BER performance of the receiver is improved by the use of LDPC channel encoder.

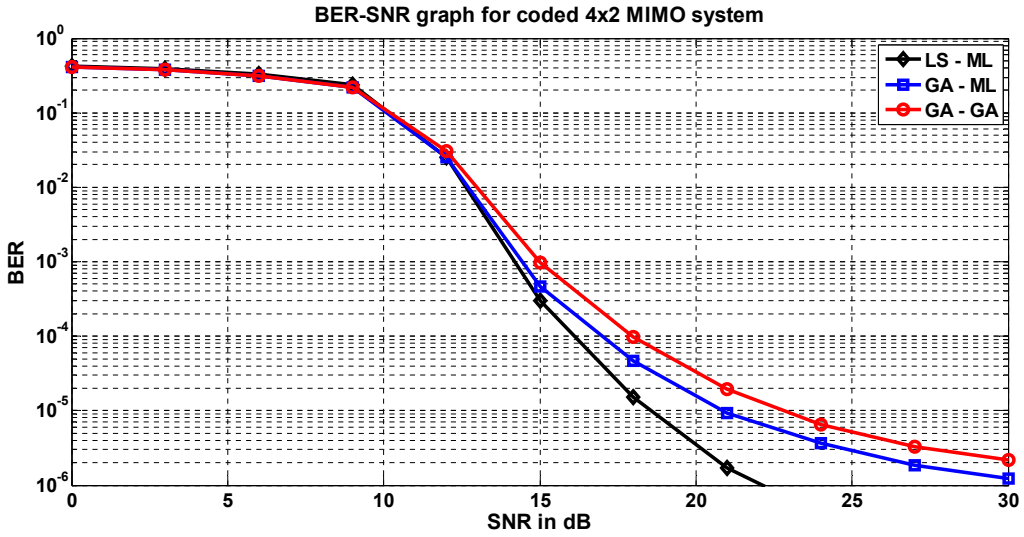

Figure 29: BER-SNR graph for JCEDD methods with channel coding.

Performance of the communication system with channel encoder is low from 0dB to 9dB and increases remarkably for SNR values greater than 9dB. GA-based JCEDD receiver with LDPC channel encoder gives BER performance of **$2.19\text{x}10^{-6}$** at **30dB**.

Table 20 shows some BER values at specific SNR points of LS-ML, GA-ML, and GA-GA JCEDD methods.

SNR	LS-ML uncoded	GA-ML uncoded	GA-GA uncoded	LS-ML coded	GA-ML coded	GA-GA coded
0	0.3672	0.3342	0.3503	0.4183	0.4078	0.4095
6	0.2836	0.2597	0.2665	0.3308	0.3167	0.3092
12	0.1760	0.1669	0.1735	0.0251	0.0255	0.0304
18	0.0734	0.0952	0.1067	$1.54\text{x}10^{-5}$	$4.63\text{x}10^{-5}$	$9.87\text{x}10^{-5}$
24	0.0317	0.0566	0.0659	$4.28\text{x}10^{-7}$	$3.70\text{x}10^{-6}$	$6.58\text{x}10^{-6}$
30	0.0038	0.0230	0.0361	$1.43\text{x}10^{-7}$	$1.23\text{x}10^{-6}$	$2.19\text{x}10^{-6}$

Table 20: BER values of JCEDD methods at specific SNR values.

Comparison of performance of coded and uncoded JCEDD methods is given on Figure 30. Receivers with channel encoder gives relatively great performance compared to receivers without channel encoder.

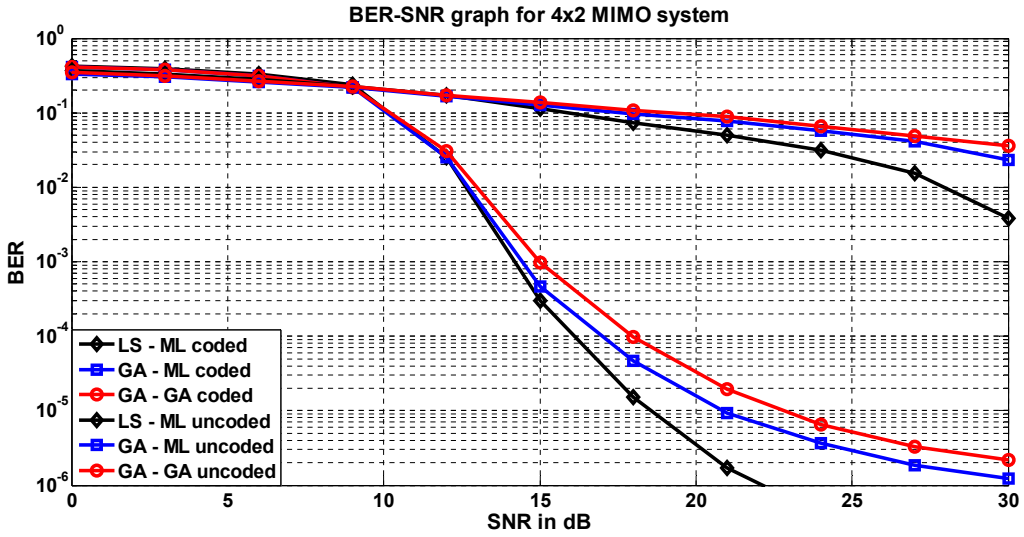

Figure 30: Comparision of JCEDD methods with and without coding.

BER performance of GA-GA, GA-ML, and LS-ML JCEDD methods increase from **0.1067**, **0.0952**, and **0.0734** to **$9.87\text{x}10^{-5}$**, **$4.63\text{x}10^{-5}$**, **$1.54\text{x}10^{-5}$** respectively at **18dB**.

6.3 Complexity Analysis

Computational complexity of CE and MUD methods are analyzed based on the number of mathematical calculations performed per each estimation stage. Number of computation performed in each operation of GA-based CE and GA-based MUD methods are given in Table 21 and Table 22 respectively.

GA-based CE operator	No of additions	No of subtractions	No of multiplications	No of divisions	No of power calculations	No of comparison
Selection	24Xp	8Xp	32Xp	0	8Xp	Xp
Crossover	0.8Xp	0	0	0.8Xp	0	0
Mutation	4.8Xp	4.8Xp	0	0	0	0
Replacement	242.4Xp	80.8Xp	323.2Xp	0	80.8Xp	10.1Xp
Total	272Xp	93.6Xp	355.2Xp	0.8Xp	88.8Xp	11.1Xp

Table 21: Number of computations performed in GA-based CE operators.

GA-based MUD operator	No of additions	No of subtractions	No of multiplications	No of divisions	No of power calculations	No of comparison
Selection	6Nx	2Nx	8Nx	0	2Nx	Nx
Crossover	0	0	0	0	0/0	0
Mutation	0	0	0	0	0/0	0.1Nx
Replacement	1.8Nx	0.6Nx	2.4Nx	0	0.6Nx	0.3Nx
Total	7.8Nx	2.6Nx	10.4Nx	0	2.6Nx	1.4Nx

Table 22: Number of computations performed in GA-based MUD operators.

Total number of individuals used as an input per estimation for GA-based CE and GA-based MUD methods are **16,380** and **33,000** respectively. Total number of computations per estimation is given in Table 23.

CE or MUD Method	No of additions	No of subtractions	No of multiplications	No of divisions	No of power calculations	No of comparison
GA – CE	4,455,360	1,533,168	5,818,176	13,104	1,454,544	181,818
GA – MUD	257,400	85,800	343,200	0	85,800	46,200
ML – MUD	393,216	131,072	524,288	0	131,072	65,536

Table 23: Computational analysis of CE and MUD methods

From Table 23 GA-based MUD decreases computational complexity of ML method by decreasing total number of individuals analyzed from **65,536** to **42,900** and total number of computations from **1,245,184** to **818,400**.

CHAPTER 7

CONCLUSIONS AND RECOMMENDATIONS

7.1 Conclusions

The number of users supported by a basestation, as a result capacity of a cellular system, can be increased by using MU-MIMO technology. For uplink MU-MIMO system with four simultaneous mobile users and two receiver antennas at the basestation, GA-based JCEDD is designed at the receiver for channel estimation and multi-user detection.

GA-based CE is designed with optimum parameter values of Xp=800, Xr=20, Y_{Tot}=40, and Xrt=0.2. BER and MSE performance of GA-based CE is greater than other CE methods for SNR values between 0 and 12dB and this makes the estimator highly robust for low SNR communication systems.

GA-based MUD method is developed for optimum parameter values of Nx=30000, Ny=2, Ns=0.1Nx, and Nr=0.1 which gives total individuals of 42900. BER and MSE performance of GA-based MUD is the same as that of ML for 0-15dB SNR values and as SNR increases its relative performance decreases. GA-based MUD decreases computational complexity of ML detector by **22,636** individuals or by **426,784** computations.

GA-based JCEDD is constructed from GA-based CE and GA-based MUD and it gives BER performance of a little less than of LS-ML methods. Finally use of LDPC channel encoder increases the performance of the basestation receiver from **0.1067**, **0.0952**, and **0.0734** BER values to **9.87×10^{-5}**, **4.63×10^{-5}**, and **1.54×10^{-5}** respectively at **18dB.**

Generally GA-based methods give relatively good results for optimization problems with many variables, overloaded basestation receivers, and communication systems at low SNR environment. GA-based JCEDD gives a promising result for future wireless technologies.

7.2 Recommendations for Future Work

Design of uplink MU-MIMO cellular system is based on Rayleigh flat fading channel. If the channel is changed to frequency selective fast fading channel, then the communication system designed with OFDM technology. This will increase the number of subcarriers and as a result the relative performance of GA-based CE algorithm increases.

As current and future wireless technologies require high speed data transmission, use of higher order modulation techniques is a requirement. This increases complexity of the data detectors like ML method. GA will decrease computational complexity and will be a good choice for communications with a high modulation order.

From the nature of the overloaded system the diversity gain of the received data is so much low and it decreases the performance of the receiver. Addition of cooperative nodes or increasing number of antennas per mobile user increases the diversity of the overloaded receiver system.

As SNR increases above 15dB, relative performance of genetic algorithms decreases due to interuser interferences between simultaneous users. To overcome this problem space-time coding should designed at the system.

References

[1] A. Goldsmith, *Wireless Communications*, 1st Edition. New York: Cambridge University Press, 2005.

[2] X. Wang and H. V. Poor, *Wireless Communication Systems: Advanced Techniques for Signal Reception*, 1st Edition. New York: Prentice Hall, 2003.

[3] T. Rappaport, *Wireless Communications Principles and Practice*, 2nd Edition. New York: Prentice Hall, 2001.

[4] A. F. Molisch, *Wireless Communications*, 2nd Edition. United Kingdom: John Wiley & Sons Ltd, 2011.

[5] S. G. Glisic, *Advanced Wireless Communications: 4G Cognitive and Cooperative Broadband Technology*, 2nd Edition. United Kingdom: John Wiley & Sons Ltd, 2007.

[6] J. G. Proakis, *Digital Communications*, 4th Edition. New York: McGraw Hill, 2000.

[7] A. Sibille, et al., *MIMO: From Theory to Implementation*, 1st Edition. United Kingdom: Elsevier Inc, 2011.

[8] E. Biglieri, et al., *MIMO Wireless Communications*, 1st Edition. New York: Cambridge University Press, 2007.

[9] D. Tse and P. Viswanath, *Fundamentals of Wireless Communication*, 1st Edition. New York: Cambridge University Press, 2005.

[10] F. D. Flaviis, et al., *Multi-antenna Systems for MIMO Communications*, 1st Edition. New York: Morgan & Claypool Publishers, 2008.

[11] G. Tsoulos, *MIMO System Technology for Wireless Communications*, 1st Edition. New York: CRC Press, 2006.

[12] Y. S. Cho, et al., *MIMO-OFDM Wireless Communications with MATLAB*, 1st Edition. Singapore: John Wiley & Sons (Asia) Ltd, 2010.

[13] L. Hanzo, et al., *MIMO-OFDM for LTE, Wi-Fi and WiMAX Coherent versus Non-coherent and Cooperative Turbo-transceivers*, 1st Edition. United Kingdom: John Wiley & Sons Ltd, 2011.

[14] H. K. Bizaki, *MIMO Systems, Theory and Applications*, 1st Edition. India: Intech Open Access Publisher, 2011.

[15] M. L. Honig, *Advances in Multiuser Detection*, 1st Edition. New Jersey: John Wiley & Sons Inc., 2009.

[16] G. E. Bottomley, *Channel Equalization for Wireless Communications from Concepts to Detailed Mathematics*, 1st Edition. New Jersey: John Wiley & Sons Inc., 2011.

[17] S. N. Sivanandam and S. N. Deepa, *Introduction to Genetic Algorithms*, 1st Edition. New York: Springer-Verlag Berlin Heidelberg, 2008.

[18] R. L. Haupt and S. E. Haupt, *Practical Genetic Algorithms*, 2nd Edition. New Jersey: John Wiley & Sons Inc., 2004.

[19] T. Munakata, *Fundamentals of the New Artificial Intelligence: Neural, Evolutionary, Fuzzy and More*, 2nd Edition. London: Springer-Verlag London Ltd., 2008.

[20] M. T. Jones, *Artificial Intelligence: A Systems Approach*, 1st Edition. Massachusetts: Infinity Science Press LLC, 2008.

[21] S. J. Russell and P. Norvig, *Artificial Intelligence: A modern approach*, 2nd Edition. New Jersey: Pearson Education Inc., 2003.

[22] J. Hoadley, "Building Future Networks with MIMO and OFDM". Available: http://connectedplanetonline.com/wireless/technology/mimo_ofdm_091905/.

[23] J. H. Winters, "Optimum combining in digital mobile radio with co-channel interference," *IEEE Journal on Selected Areas in Communications*, vol. 2, no. 4, pp. 528–539, July 1984.

[24] J. H. Winters, "Optimum combining for indoor radio systems with multiple users," *IEEE Transactions on Communications*, vol. 35, no. 11, pp. 1222–1230, November 1987.

[25] J. H. Winters, "On the capacity of radio communication systems with diversity in a Rayleigh fading environment," *IEEE Journal on Selected Areas in Communications*, vol. 5, no. 5, pp. 871–878, June 1987.

[26] A. F. Molisch and J. H. Winters, "Space-time-frequency (STF) coding for MIMO-OFDM systems," *IEEE Communications Letters*, vol. 6, no. 9, pp. 370-372, September 2002.

[27] A. F. Molisch and J. H. Winters, "Reduced-complexity transmit/receive-diversity systems," *IEEE Transactions on Signal Processing*, vol. 51, no. 11, pp. 2729 – 2738, November 2003.

[28] R. S. Blum and J. H. Winters, "On optimum MIMO with antenna selection," *IEEE Communications Letters*, vol. 6, no. 8, pp. 322 – 324, August 2002.

[29] Y. G. Li, et al., "MIMO-OFDM for wireless communications: signal detection with enhanced channel estimation," *IEEE Transactions on Communications*, vol. 50, no. 9, pp. 1471-1477, September 2002.

[30] M. Z. Win and J. H. Winters, "Analysis of hybrid selection/maximal-ratio combining in Rayleigh fading," *IEEE Transactions on Communications*, vol. 47, no. 12, pp. 1773-1776, December 1999.

[31] G. J. Foschini, "Layered space-time architecture for wireless communication in a fading environment when using multi-element antennas," *Bell Labs Technical Journal*, pp. 41–59, 1996.

[32] G. J. Foschini and M. J. Gans, "On limits of wireless communications in a fading environment when using multiple antennas," *Wireless Personal Communications*, vol. 6, pp. 311–335, March 1998.

[33] G. J. Foschini, et al., "Simplified processing for high spectral efficiency wireless communication employing multi-element arrays," *IEEE Journal on Selected Areas in Communications*, vol. 17, no. 11, pp. 1841–1852, November 1999.

[34] H. Liu and G. Xu, "Smart antennas in wireless systems: uplink multiuser blind channel and sequence detection," *IEEE Transactions on Communications*, vol. 45, no. 2, pp. 187–199, February 1997.

[35] I. Bradaric, et al., "Blind MIMO FIR channel identification based on second-order spectra correlations," *IEEE Transactions on Signal Processing*, vol. 51, pp. 1668–1674, June 2003.

[36] J. Xavier, et al., "Closed-form correlative coding (CFC2) blind identification of MIMO channels: isometry fitting to second order statistics," *IEEE Transactions on Signal Processing*, vol. 49, no. 5, pp. 1073–1086, May 2001.

[37] Y. Li, "Simplified channel estimation for OFDM systems with multiple transmit antennas," *IEEE Transactions on Wireless Communications*, vol. 1, no. 1, pp. 67–75, January 2002.

[38] I. Barhumi, et al., "Optimal training design for MIMO OFDM systems in mobile wireless channels," *IEEE Transactions on Signal Processing*, vol. 51, pp. 1615–1624, June 2003.

[39] M. Shin, et al., "Enhanced channel-estimation technique for MIMO-OFDM systems," *IEEE Transactions on Vehicular Technology*, vol. 53, no. 2, pp. 262–265, January 2004.

[40] K. J. Kim, et al., "A QRD-M/Kalman filter-based detection and channel estimation algorithm for MIMO-OFDM systems," *IEEE Transactions on Wireless Communications*, vol. 4, no. 2, pp. 710–721, March 2005.

[41] H. Minn, et al., "A reduced complexity channel estimation for OFDM systems with transmit diversity in mobile wireless channels," *IEEE Transactions on Communications*, vol. 50, no. 5, pp. 799–807, May 2002.

[42] Increasing capacity in wireless broadcast systems using distributed transmission/directional reception (DTDR), by T. Kailath and A. J. Paulraj. (1994, September 6). Patent US5345599 A [Online]. Available: http://www.google.com/patents/US5345599.

[43] Spatial division multiple access wireless communication systems, by B. Ottersten, R. H. Roy. (1996, May 7). Patent US5515378 A [Online]. Available: http://www.google.com/patents/US5515378.

[44] L. H. Brandenburg and A. D. Wyner, "Capacity of the Gaussian channel with memory: the multivariate case," *Bell Labs Technical Journal*, vol. 53, no. 5, pp. 745–778, June 1974.

[45] G. D. Golden, et al., "Detection algorithm and initial laboratory results using V-BLAST space–time communication architecture," *IEEE Electronic Letters*, vol. 35, pp. 14–16, January 1999.

[46] "Multiple-input multiple-output communications," Wikipedia.org [Online]. Available: http://en.wikipedia.org/wiki/Multiple-input_multiple-output_communications.

[47] Z. Wang, et al., "A MIMO-OFDM channel estimation approach using time of arrivals," *IEEE Transactions on Wireless Communications*, vol. 4, pp. 1207–1213, May 2005.

[48] Y. Zeng and T. S. Ng, "A semi-blind channel estimation method for multi-user multi-antenna OFDM systems," *IEEE Transactions on Signal Processing*, vol. 52, pp. 1419–1429, May 2004.

[49] S. Thoen, et al., "Constrained least squares detector for OFDM/SDMA-based wireless networks," *IEEE Transactions on Wireless Communications*, vol. 2, pp. 129–140, January 2003.

[50] F. W. Vook and T. A. Thomas, "MMSE multi-user channel estimation for broadband wireless communications," *IEEE Global Telecommunications Conference (GLOBECOM'01)*, vol. 1, pp. 470–474, November 2001.

[51] S. S. Moghaddam and H. Saremi, "A Novel Semi-blind Channel Estimation Scheme for Rayleigh Flat Fading MIMO channels (joint LS estimation and ML detection)" Available: http://www.jr.ietejournals.org/article.asp?issn=0377-2063;year=2010;volume=56;issue=4;spage=193;epage=201;aulast=Moghaddam.

[52] S. Verdu, *Multiuser Detection*, 1st Edition. New York: Cambridge University Press, 1998.

[53] S. Chen and Y. Wu, "Maximum likelihood joint channel and data estimation using genetic algorithms," *IEEE Transactions on Signal Processing*, vol. 46, pp. 1469–1473, May 1998.

[54] K. Yen and L. Hanzo, "Genetic algorithm assisted joint multiuser symbol detection and fading channel estimation for synchronous CDMA systems," *IEEE Journal on Selected Areas in Communications*, vol. 19, pp. 985–998, June 2001.

[55] K. Yen and L. Hanzo, "Genetic algorithm-assisted multiuser detection in asynchronous CDMA communications," *IEEE Transactions on Vehicular Technology*, vol. 53, pp. 1413–1422, September 2004.

[56] F. Ciriaco, et al., "Genetic algorithm applied to multipath multiuser channel estimation in DS/CDMA systems," *IEEE Symposium on Spread Spectrum Techniques and Applications*, vol. 9, pp. 138-142.

[57] M. Jiang, et al., "Iterative joint channel estimation and symbol detection for multi-user MIMO OFDM," *MIMO OFDM for LTE, Wi-Fi and WiMAX*, 1st Edition. United Kingdom: John Wiley & Sons Ltd, 2011, pp. 247-269.

[58] H. Ali and D. I. Amshah, "GSR: a new genetic algorithm for improving source and channel estimates," *IEEE Transactions on Circuits and Systems I*, vol. 54, no. 5, May 2007.

[59] L. Hanzo, et al., "Iterative joint channel estimation and multi-user detection for multiple-antenna aided OFDM systems," *IEEE Transactions on Wireless Communications*, vol. 6, no. 8, August 2007.

[60] J. B. Yamindi and W. Mu-qing, "The analytical method of genetic algorithm–aided iterative joint channel estimation and multi–user detection," *Australian Telecommunications Networks and Applications Conference (ATNAC)*, 2009.

[61] J. Zhang, et al., "Joint channel estimation and multi-user detection for SDMA OFDM based on dual repeated weighted boosting search," *IEEE Communications Society IEEE ICC proceedings*, 2011.

[62] D. J. Costello and S. Lin, *Error Control Coding*, 2nd Edition. United States: Pearson Education Inc, 2004.

[63] C. Moreira and G. Farrell, *Essentials of Error Control Coding*, 1st Edition. England: John Wiley & Sons Ltd, 2006.

[64] P. Sweeney, *Error Control Coding: From Theory to Practice*, 1st Edition. England: John Wiley & Sons Ltd, 2002.

[65] Y. Jiang, *A Practical Guide to Error-Control Coding Using MATLAB*, 1st Edition. United States: Artech House, 2010.

[66] T. K. Moon, *Error Correction Coding Mathematical Methods and Algorithms*, 1st Edition. New Jersey: John Wiley & Sons, Inc., 2005.